

12-2019

Effect of Fe₃O₄ Nanoparticles on Performance of Shape Memory Polymers Foam Using Solid State Foaming Process

Tamem Salah

Follow this and additional works at: https://scholarworks.uaeu.ac.ae/mechan_theses



Part of the [Engineering Commons](#)

Recommended Citation

Salah, Tamem, "Effect of Fe₃O₄ Nanoparticles on Performance of Shape Memory Polymers Foam Using Solid State Foaming Process" (2019). *Mechanical Engineering Theses*. 7.
https://scholarworks.uaeu.ac.ae/mechan_theses/7

This Thesis is brought to you for free and open access by the Mechanical Engineering at Scholarworks@UAEU. It has been accepted for inclusion in Mechanical Engineering Theses by an authorized administrator of Scholarworks@UAEU. For more information, please contact fadl.musa@uaeu.ac.ae.



جامعة الإمارات العربية المتحدة
United Arab Emirates University

United Arab Emirates University

College of Engineering

Department of Mechanical Engineering

EFFECT OF FE_3O_4 NANOPARTICLES ON
PERFORMANCE OF SHAPE MEMORY POLYMERS
FOAM USING SOLID STATE FOAMING PROCESS

Tamem Salah

This thesis is submitted in partial fulfillment of the requirements for Master in
Materials Science & Engineering

Under the Supervision of Doctor Aiman Ziout

December 2019

Declaration of Original Work

I, Tamem Salah, the undersigned, a graduate student at the United Arab Emirates University (UAEU), and the author of this thesis entitled "*Effect of Fe₃O₄ Nanoparticles on Performance of Shape Memory Polymers Foam Using Solid State Foaming Process*", hereby, solemnly declare that this thesis is my own original research work that has been done and prepared by me under the supervision of Dr. Aiman Ziout, in the College of Engineering at UAEU. This work has not previously been presented, published, or formed the basis for the award of any academic degree, diploma or a similar title at this or any other university. Any materials borrowed from other sources (whether published or unpublished) and relied upon or included in my thesis have been properly cited and acknowledged in accordance with appropriate academic conventions. I further declare that there is no potential conflict of interest with respect to the research, data collection, authorship, presentation and/or publication of this thesis.

Student's Signature: _____



Date: 30/Dec/2019

Approval of the Master Thesis

This Master Thesis is approved by the following Examining Committee Members:

- 1) Advisor (Committee Chair): Dr. Aiman Ziout

Title: Assistant Professor

Department of Mechanical Engineering

College of Engineering

Signature



Date 24/12/2019

- 1) Member (Internal Examiner): Dr. Jaber Abu Qudeiri

Title: Associate Professor

Department of Mechanical Engineering

College of Engineering

Signature



Date 23/12/2019

- 1) Member (Internal Examiner): Dr. Kassim Abdullah

Title: Associate Professor

Department of Mechanical Engineering

College of Engineering

Signature



Date 23/12/2019

- 3) Member (External Examiner): Ridha Ben Mrad

Title: Professor

Department of Mechanical and Industrial Engineering

Institution: University of Toronto

Signature



Date

26/12/2019

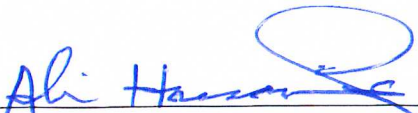
This Master Thesis is accepted by:

Dean of the College of Engineering Professor Sabah Alkass

Signature 

Date 30/12/2019

Dean of the College of Graduate Studies: Professor Ali Al-Marzouqi

Signature 

Date 30/12/2019

Copy 4 of 5

Copyright © 2019 Tamem Salah
All Rights Reserved

Abstract

The scope of this research is the emerging class of smart materials namely stimulus-responsive shape memory polymers (SMP) that can be actuated on demand to recover their original shape, after being quasi-plastically distorted. SMP are ideal for an integrated intelligent system, in which the structure is heated to a certain temperature to generate reactive motion as pre-programmed. This research aims to employ a new emerging method for generating foam structure; called solid-state foaming. The generated foamed structures are advantageous over fully dense SMP in terms of the low density, high compressibility and high deformations when they recover their permanent shape. However, the mechanical properties of these samples is reduced due to the existence of pores.

In this research, effects of polymer type, nanoparticle percentage, packing pressure, holding time, foaming temperature and foaming time parameters were tested. Two levels were selected for each factor. A Taguchi design was selected to determine number of experiments needed to be conducted. Post to foaming of the samples, their performance namely foaming ratio, shape recovery speed and actuation load were evaluated. Further characterization techniques namely Differential Scanning Calorimetry (DSC), Fourier Transformation Infrared Spectroscopy (FTIR) and X-ray Diffraction (XRD) were operated on the samples in their original form to obtain better knowledge of their structure and chemical composition. The experimental results showed that temperature has no impact on the actuation load, as long as a temperature above glass transition temperature is applied. Addition of nano-particles caused the shape recovery speed to reduce; due to creation of discontinuity within the polymer matrix. However, higher foaming ratio was obtained when NPs were introduced to the polymer structure.

Keywords: Shape Memory Effect, Shape Memory Polymer, Epoxy Foam, Nano Composites, Iron Oxide Nanoparticles, Fillers.

Title and Abstract (in Arabic)

تأثير جسيمات أكسيد الحديد النانوية على أداء اللدائن الرغوية حافظة الشكل باستخدام عملية رغوة الحالة الصلبة

المخلص

نطاق هذا البحث هو فئة ناشئة من المواد الذكية وهي اللدائن حافظة الشكل و المستجيبة للحوافز (SMP) التي يمكن تشغيلها عند تقديم المحفز الصحيح لاستعادة شكلها الأصلي، بعد أن يتم تشويه شكلها الاصيلي للشكل الثانوي. هذه المواد هي مثالية لنظام ذكي متكامل، حيث يتم تسخين هيكلها إلى درجة حرارة معينة لتوليد حركة تفاعلية معرفة مسبقاً. يهدف هذا البحث إلى توظيف طريقة جديدة انتاج عينات ذات بنية رغوية؛ هذه الطريقة تدعى رغوة الحالة الصلبة. تتميز الهياكل الرغوية المنتجة بميزة مقارنة بالعينات الأصلية ذات الكثافة العالية من حيث الكثافة المنخفضة، قابلية الانضغاط العالي والتشوهات العالية عند استعادة شكلها الدائم. ومع ذلك، تعتبر الخواص الميكانيكية لهذه العينات اقل كفاءة بسبب وجود المسامات فيها.

في هذا البحث، تم اختبار تأثير عوامل مختلفة على هذه العملية مثل: نوع اللدن، نسبة الجسيمات النانوية، الضغط المطبق على العينة، مدة تطبيق الضغط، درجة حرارة الفرن و وقت الرغوة. تم اختيار مستويين لكل عامل من هذه العوامل. تم تصميم خريطة Taguchi لتحديد عدد التجارب اللازمة للوصول لنتائج موثوقة. بعد عملية انشاء عينات رغوية، تم تقييم أدائها من خلال حساب نسبة الرغوة، سرعة استعادة الشكل و قوة الدفع المطبقة. تم إجراء مزيد من الدراسات على العينات في شكلها الأساسي للوصول لمعرفة أفضل لبنيتها و تركيبها الكيميائي، الدراسات الاختبارات تمت عن طريق استخدام: قياس الكالوري التفرسي التفرقي (DSC)، التحليل الطيفي للأشعة تحت الحمراء (FTIR) و تقنية حيود الأشعة السينية (XRD). النتائج التجريبية أظهرت أن درجة الحرارة لا تؤثر على قوة الدفع المطبقة من قبل العينات، طالما أنه يتم تطبيق درجة حرارة أعلى من درجة حرارة التحول الزجاجي. تسبب إضافة الجزيئات النانوية في تقليل سرعة استعادة الشكل؛ بسبب إنشائها فجوات داخل جسم العينة. ومع ذلك، تم الحصول على نسبة رغوة أعلى عند إدخال تلك الجسيمات في بنية العينة اللدنة.

مفاهيم البحث الرئيسية: تأثير شكل الذاكرة، بوليمرات ذات الذاكرة، رغوة الايبوكسي، مركبات نانوية، جسيمات أكسيد الحديد النانوية، الحشو.

Acknowledgements

“Praise Allah, who has guided us to this; and we would never have been guided if Allah had not guided us” [Quran 7:43]. All thanks to Mighty Allah for guiding me through this master program and research, without him I would not have been able to move forward.

I would like to thank the committee who were always there for me whenever I faced any issue, for guiding me, and for supporting me throughout my preparation of this thesis. I would like to thank Dr. Aiman Ziout of the Mechanical Engineering Department at the United Arab Emirates University as an academic supervisor for guiding me and supporting me during my master studies and research to finish it all well.

Special thanks are extended to my family for their support and friendship. Big special thanks to my parents for guiding me in hard times whenever needed.

I would also like to praise myself for the dedication, hard work and continuous effort in order to achieve my goal and to publish a research that can help researchers and publisher at best.

Dedication

To myself and my beloved family

Table of Contents

Title	i
Declaration of Original Work	ii
Copyright	iii
Advisory Committee	iv
Approval of the Master Thesis	v
Abstract	vii
Title and Abstract (in Arabic)	viii
Acknowledgements	ix
Dedication	x
Table of Contents	xi
List of Tables.....	xiv
List of Figures	xv
List of Abbreviations.....	xvi
Chapter 1: Introduction	1
1.1 Background	1
1.2 Research Question.....	2
1.3 Methodology	2
1.4 Expected Outcomes and Impact.....	3
1.5 Limitation of the Research	3
1.6 Thesis Structure.....	4
Chapter 2: Literature Review and Background.....	5
2.1 Polymers.....	5
2.1.1 Polymerization Process	5
2.1.2 Properties of Polymers	6
2.2 Fillers.....	7
2.2.1 Fe ₃ O ₄ Properties	8
2.2.2 Fe ₃ O ₄ Synthesis and Preparation Methods.....	10
2.2.2.1 Co-precipitation Preparation	10
2.2.2.2 Combustion Method	11
2.2.3 Fe ₃ O ₄ Applications	11
2.3 Shape Memory Effect	11
2.3.1 Shape Memory Polymers (SMPs)	13
2.3.2 Shape Memory Foam	14
2.3.3 Shape Memory Polymer Composites	17

2.4 Applications of Shape Memory Polymers	20
2.5 Critical Review.....	22
Chapter 3: Experimental Methods	23
3.1 Sample Preparation	23
3.1.1 Nanoparticles Preparation	23
3.1.1.1 X-ray Diffraction (XRD).....	23
3.1.2 Selection of Polymers.....	25
3.1.2.1 Functional Group Analysis.....	26
3.2 Design of Experiment	27
3.3 Foaming Process Procedures.....	30
3.4 Measurements	36
3.4.1 Foaming Ratio	36
3.4.2 Shape Memory Effect.....	37
3.4.3 Actuation Load	38
3.4.4 Optimum Processing Parameters.....	39
3.5 Sample Characterization	40
Chapter 4: Optimizing Foaming Process	42
4.1 Process Model	42
4.2 Process Parameters.....	43
4.2.1 The Determination of Foaming Temperature.....	43
4.2.2 Nanoparticles Percentage	45
4.2.3 Packing Pressure.....	45
4.2.4 Holding Time.....	46
4.2.5 Foaming Time	46
4.3 Foaming Ratio and Density Measurements	46
4.4 Data Analysis	47
4.5 Confirmation Experiment.....	50
Chapter 5: Optimizing Performance	52
5.1 Optimizing Shape Memory Effect	52
5.1.1 Optimal Shape Memory Effect Based on Taguchi Design	53
5.2 Optimizing Actuation Load.....	54
5.2.1 Relationship between Actuation Load and Sample Length	56
5.2.2 Optimal Actuation Load Based on Taguchi Design.....	57
5.3 Optimum Processing Parameters	59
Chapter 6: Discussion	61
6.1 Foaming Temperature Determination	61
6.2 Foaming Ratio and Density Measurements	66
6.2.1 Optimal Ratio and Density Based on Taguchi Design.....	67
6.2.2 Modified Optimal Suggested by Taguchi.....	68
6.3 Shape Memory Effect	68
6.3.1 Optimal Shape Memory Effect Based on Taguchi Design.....	70

6.4 Actuation Load Measurement	71
6.5 Overall Optimum Processing Parameters	74
Chapter 7: Conclusion.....	76
References	78

List of Tables

Table 1: Taguchi map designed for this research.....	30
Table 2: Average calculated foaming ratio and average foam density for each set of experiment	47
Table 3: Response table for foam density means	50
Table 4: Response table for foaming ratio means	50
Table 5: Results of the configuration experiment using parameters recommended by Taguchi analysis	51
Table 6: Average calculated values for recovery speed and time for each experiment.....	52
Table 7: Average measured actuation load values for every experiment.....	54
Table 8: Response table for actuation load means	56
Table 9: Values of foaming ratio, density, recovery speed and actuation load of tablets prepared under optimum levels.....	60
Table 10: Taguchi design of process parameter for optimal ratio and density	68
Table 11: Effect of NP% on the recovery speed (mm/minute).....	69
Table 12: Effect of packing pressure on the recovery speed	70
Table 13: Taguchi design of process parameter for optimal SME.....	71
Table 14: Selected optimum parameters levels.....	75

List of Figures

Figure 1: Crystal structure of Fe_3O_4	9
Figure 2: One-way vs two-way SME.....	13
Figure 3: Shape memory effect steps in polymers	14
Figure 4: XRD pattern of the prepared nanoparticles	24
Figure 5: Comparison between the prepared and the standard Fe_3O_4	25
Figure 6: FTIR bands of pure PE sample.....	27
Figure 7: Process parameters and responses	29
Figure 8: Stainless steel mold containing the powder that is to be packed using the hydraulic press machine	32
Figure 9: A mold used to insert the sample inside the furnace for foaming process.....	34
Figure 10: Prepared tablet inserted inside a thick aluminum sheet and a mold on a stainless-steel base ready to be foamed	34
Figure 11: A Samples after the foaming process and removal from the oven, ready to be extracted from the molds.....	35
Figure 12: Samples being machined and shaped into auniformed shape for easier calculations using a CNC machine.....	36
Figure 13: A sample just heated, compressed to 50%, recovered its original height.....	38
Figure 14: A graph generated using data extracted from MESUR Life software and the force gauge	39
Figure 15: Process model of this research.....	42
Figure 16: Foam ratios as a function of temperature for pure PE and PE+2% NPs	44
Figure 17: Foam ratios as a function of temperature for pure JSD and JSD+2% NPs	44
Figure 18 Irregular sample foamed at 0 LBS packing pressure.....	45
Figure 19: Effect of all parameters on foam density.....	48
Figure 20: Effect of all parameters on foaming ratio.....	49
Figure 21: Effect of all parameters on recvery speed of samples	53
Figure 22: Effect of all parameters on the actuation load	55
Figure 23: Actuation load curves for each experiment	59
Figure 24: DSC run of Pure JSD.....	62
Figure 25: DSC run of pure PE.....	63
Figure 26: DSC graph of JSD + 2 w.t% Fe_3O_4	64
Figure 27: DSC graph of PE + 0.5 w.t% Fe_3O_4	64
Figure 28: Shape recovery time or PE polymer at different NPs concentrations.....	65
Figure 29: Stress strain graph for both pure PE and pure JSD.....	72
Figure 30: Effect of NPs addition on the compressibility of the samples.....	72
Figure 31: Foamed samples	73

List of Abbreviations

\overline{M}_n	Number average molecular weight
\overline{M}_w	Weight average molecular weight
\bar{Y}_1, \bar{Y}_2	Samples mean
$N_{Taguchi}$	Number of experiments
N_v	Number of parameters
s_1^2, s_2^2	Samples variance
BPO	Benzoyl peroxide
CNTs	Carbon nanotubes
Co_3O_4	Cobalt(II,III) Oxide
DSC	Differential scanning calorimeter
EMI	Electromagnetic interference shielding
$Fe(NO_3)_3$	Iron(III) nitrate
$Fe(OH)_3$	Iron(III) oxide-hydroxide
Fe^{+2}	Ferrous
Fe^{+3}	Ferric
Fe_3O_4	Iron Oxide
$FeCl_2$	Iron(II) chloride
$FeCl_3$	Iron(III) chloride
$FeSO_4$	Iron(II) sulfate
FTIR	Fourier transform infrared

GO	Graphene oxide
IONPs	Iron oxide nanoparticles
JSD	Jotun super durable 2903
KNO ₃	Potassium nitrate
KOH	Potassium hydroxide
LBS	Pounds
MMT	Nano-clay particles
MNPs	Magnetic nanoparticles
MRI	Magnetic resonance imaging
N ₁ , N ₂	Sample size
NaOH	Sodium hydroxide
NPs	Nano-particles
PCL	Poly-epsilon- caprolactone
PDLLA	Poly(d,l-lactide)
PE	Corro-Coat PE Series 7
PEG	Polyethylene glycol
PI	Polyimide
PLA	Poly(lactic-acid)
PMMA	Poly(methyl methacrylate)
SF	Silk fibrin
SiC	Silicon carbide
SMP	Shape memory polymer

SMPU	Shape memory polyurethane
T_g	Glass transition temperature
TGIC	Triglycidyl isocyanurate
T_m	Melting temperature
T_{perm}	Permanent temperature
T_{trans}	Transition temperature
wt. %	Weight percentage
XRD	X-ray diffractometer
α -Fe ₂ O ₃	Hematite
γ -Fe ₂ O ₃	Maghemite
D	Crystal size
K	Sherrer's constant
L	Number of levels
M_i	Molecular weight
N_i	Number of molecules
W_i	Weight of the molecule
β	Full width at half maximum

Chapter 1: Introduction

1.1 Background

Stimulus responsive shape memory materials can recover their original shape after they have been distorted by an external factor. Shape Memory Polymers (SMPs) are widely used for aerospace applications due to their unique properties such as their transparency, low cost, ease of processing, shape recovery ratio and their light weight. Indeed, SMPs can be turned into foam with a porous structure leading to lower overall densities and a lower storage volume in a compressed state; however, due to the lower density, the mechanical properties are not as good as in the SMP itself. SMP foam has an original shape and a temporary shape. At a temperature above T_{perm} , the polymer becomes rubbery and its foamed structure returns to its original shape, whereas at T_{trans} the temporary shape is apparent. Foam structure can be produced via a chemical process (Matuana, Faruk & Diaz, 2009) or a physical process (Ito et al., 2014). These processes are usually complex as they require blowing agents, complex processing steps to form the foam.

A novel method for generating foam simply and at a low cost was suggested by Quadrini and Squeo (2008). They used an epoxy resin polymer. This process began by compacting the epoxy powder into cylindrical tablets; the tablets are then heated in a muffle at a temperature higher than the boiling point of the epoxy in order to generate foam; However, this process still needs more in-depth study and exploration because many different factors may influence foam generation. These factors include packing pressure, holding time, foaming temperature, foaming time, and if fillers such as nano-particles (NPs) are to be added to the polymer powder.

In this research, inorganic metallic NPs are introduced into the structure of shape memory polymer foam, and their effect on the foaming process and the shape memory behavior is studied. These NPs are expected to enhance heat transfer ability when exposed to heat source. Zheng et al. (2009) and Wang, Ye and Tian (2016) both studied the effect of adding Fe_3O_4 NPs to different SMPs. They found that the introduction of the NPs into the shape memory polymer matrix ensured heat generation in the structure of the SMP and improved shape memory properties.

1.2 Research Question

In this research different factors that impact solid state foaming process will be studied and their effect will be determined by using Taguchi experiment design to run multiple tests. The effect of each of these factors on the produced foam ratio, density, shape recovery speed and actuation of the samples will be determined.

1.3 Methodology

The method applied will synthesize Fe_3O_4 nanoparticles via chemical co-precipitation of Fe^{2+} and Fe^{3+} ions. The synthesized Fe_3O_4 NPs will be characterized via X-ray Diffractometer (XRD) in order to obtain the sample patterns. Polymer powder's heat capacity will be determined using thermal analysis Differential Scanning Calorimeter (DSC). Fourier Transform Infrared spectroscopy (FTIR) will be operated to study the chemical composition of the polymer powder. Prior characterizing the material, shape memory foam will be produced through solid-state foaming process. The polymer powder and the NPs will be compacted together in a stainless-steel mold and foamed in an oven. The prepared samples then

will go through shape learning process and will be tested for both shape memory effect as well as actuation load.

1.4 Expected Outcomes and Impact

The goal of this research is to produce a shape memory polymer composite foam with high ratio, low density, fast shape recovery speed and a high actuation load, while using the optimum process parameters, which have been derived after conducting experiments using the Taguchi design method. This research aims to a better understanding of how different factors influence the generation of SMP foam produced by using resin powder and a solid-state foaming process. This study also aims to produce SMP foam via a simple and cost-effective method. We believe that such an SMP foam will have suitable capabilities and tailor-made properties that can be used in different fields such as aerospace and drug delivery.

1.5 Limitation of the Research

There are some limitations to this study. Firstly, a solid-state foaming process is still considered as uncontrolled because of the variable nature of pore size, bubble implementation and foam stabilization. Secondly, the parameters used here only work for polyester-based resin polymer powders. Lastly, heat transfer within the polymer matrix is only evident after exposing the foamed sample to heating and does not show any shape memory behavior when triggered by an alternating magnetic field.

1.6 Thesis Structure

The structure of this thesis is as follows. The first chapter introduces the research, its objectives, the methodology, expected outcomes and/ or impact of the study and its limitations. Chapter Two critically reviews the salient literature review and present background information on polymers, filler, shape memory foam, the foaming process and the various applications of shape memory polymers.

Chapter Three then describes the experiment and discuss in detail the sample and tablet preparation, the experimental design, sample characterization, foaming, machining and the measurements utilized in this research. The process model, its parameters, foam ratio calculations, the selections of level and confirmation experiments is described in Chapter Four.

Optimizing performance is covered in Chapter Five, which also deals with the results of shape recovery speed, actuation load tests and the optimization of the process parameters. Discussion of the results constitutes Chapter Six, including a discussion of the measurements used and the optimum process parameters. The last chapter concerns itself with the conclusions draw and the direction of future research.

Chapter 2: Literature Review and Background

2.1 Polymers

Polymers are long chains of molecules made up of small building blocks called monomers. There are two different types of polymers, thermoplastic and thermoset polymers. Thermoplastic polymers such as polyethylene can be reshaped because they have the ability to melt and flow plenty of times. On the other hand however, thermoset polymers such as resins cannot be reshaped, they are insoluble, non-melting, one gigantic molecule and they can only swell in solvents. Polymers can be formed through a process called polymerization which is basically covalently bonding many monomers together. If we are to talk about polymers structure then we have the repeating unit (mentioned before as monomers), the end group which is a structural unit that can terminate the polymer chain or in some cases can help the polymer to grow bigger, only in that case we call it a living polymer which contains a reactive end group capable of undergoing polymerization usually by heating to form a longer chain and a network polymer. The conventional polymer structure can be either linear, branched or crosslinked (network), whereas the unconventional structure includes star, comb, ladder, or stepladder structures. There are different mechanistic classifications of polymerization: step-growth and chain-growth.

2.1.1 Polymerization Process

In step-growth polymerization it is considered as a condensation reaction which forms byproducts while connecting the chains and the species grow step by step. The bonds are formed one at a time and usually the resultant polymer has a wide molecular weight distribution due to the fact that this mechanism has no

termination step and thus the end group will keep reacting until all functional groups are consumed. Examples of step-growth polymers are polyesters, polyamides, Nylon6-6 and poly-(ethylene terephthalate).

On the other hand, Chain-growth polymerization generally has three main steps: Firstly, the chain initiation step where high reactive species are generated like free radicals. Secondly, Chain propagation step where monomers keep bonding to the end group of a growing chain. Third and last step is chain termination when the polymer stops growing as two different reactive groups attach to each other or when all active end groups are consumed. In chain growth polymerization, no byproducts are formed, and the molecular weight increases rapidly. Examples of chain-growth polymers are polycaprolactone, polyethylene and polypropylene.

2.1.2 Properties of Polymers

Polymers have very wide range of physical properties that make them applicable in many different industrial fields like plastics, fibers, adhesives and coatings. Due to wide range of viscosities and electrical conductivities in polymers, they find their way into many applications like information technology, computer industries, and many other industries. These physical properties of polymers can be determined by the molecular weight. Properties like toughness and viscosity are proportional to molecular weight of the polymer.

Molecular weight is expressed using different indicators: number average, weight average, Z-average, and viscosity average molecular weight. Number average molecular weight is sensitive to total number of molecules of the polymer in a solution and is determined by end group analysis and colligative properties like

freezing point depression, boiling point elevation and osmotic pressure, it can be calculated using the below equation

$$\overline{M}_n = \frac{\sum NiMi}{\sum Ni}$$

Where Ni number of molecules, and Mi is the molecular weight of that molecule.

Weight average molecular weight on the other hand, is sensitive to the mass of molecules in a solution, and it can be determined by the light scattering and ultracentrifugation techniques, it can be calculated using the following equation:

$$\overline{M}_w = \frac{\sum WiMi}{\sum Wi}$$

Where Wi refers to the weight of the molecule.

2.2 Fillers

Fillers are considered as solid materials that are added to the polymer's matrix/structure using different methods. They are added to enhance its thermal, electrical, optical and mechanical properties either by surface interaction with the matrix or by its own physical characteristics. Carbon nanotubes, clays, glass fibers and carbon fibers are considered one of the most leading fillers. Polymer/filler composites have been widely used in various areas. A good performance is guaranteed if the polymer matrix and the filler have good interfacial interference (Taguet et al., 2014). Reducing the cost of the polymers and keeping their properties untouched or in some cases enhancing some of them in expense of others is achievable by the addition of fillers. Modification of these properties can be achieved either during or post polymerization by introducing additives or other polymers to

one polymer's matrix. Additives like plasticizers, fibers, thermal stabilizers and light stabilizers, antioxidants and flame retardants result in an enhanced polymer composites.

It is very difficult to find one classification of fillers as there is no actual one set of classifications for fillers' categories. Though, people classify fillers based on different points of view like chemical origins such as: minerals, glass, carbon black, organic, metal, etc... Others prefer to classify them according to their important properties including distribution of filler into the material's matrix, aspect ratio which is ratio of width to height, chemical composition of the surface, mechanical properties of the filler, electrical and thermal conductivity, interaction with the material (polymer) and optical properties.

Size, shape and dispersion of the filler are very important and affect the properties of the material added to it (Wypych, 2016). The radius of the filler used need to be in the same order of magnitude as the gyration radius of the polymer (Taguet et al., 2014). There are various possible shapes of fillers such as: platelets, fibers, irregular, cubical and spheres. The size of these fillers may vary from few nanometers (nano-fillers) to tens of millimeters (fibers).

2.2.1 Fe₃O₄ Properties

There are different types of Iron oxide nanoparticles (IONPs), and any type of these NPs can be obtained from the other types through oxidizing or reducing the annealing treatment. Thus, people use XRD patterns to characterize and determine the crystal structure and type of magnetic IONPs (Wu et al., 2015).

There are eight known types of iron oxides, among which there is hematite (α - Fe_2O_3), maghemite (γ - Fe_2O_3) and magnetite (Fe_3O_4). Each of these three has its unique biochemical, magnetic, catalytic, and other properties (Cornell et al., 2003).

Fe_3O_4 has the face centered cubic spinel structure that consists of a cubic close packed array of oxide ions, where all of the divalent Fe^{2+} (ferrous) ions occupy half of the octahedral sites and the trivalent Fe^{3+} (ferric) are split evenly across the remaining octahedral sites and the tetrahedral sites as shown in Figure 1. Also, Fe_3O_4 has the lowest resistivity among iron oxides due to its small band-gap (0.1 eV) as well as low toxicity (Boxall, Kelsall, & Zhang, 1996).

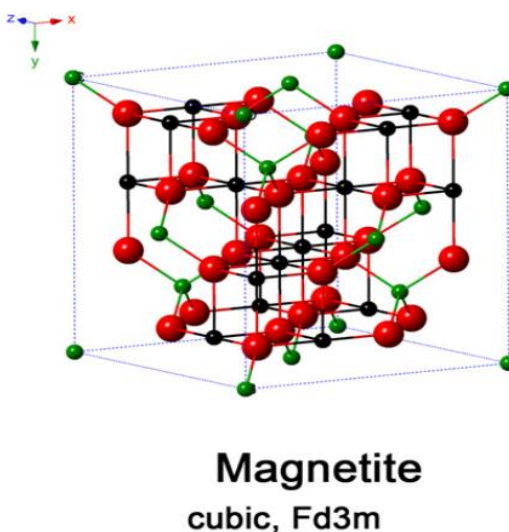


Figure 1: Crystal structure of Fe_3O_4

(Kim et al. 2015)

In general, IONPs become super-paramagnetic at room temperature when the size of IONPs is below about 15 nm, meaning that the thermal energy can overcome the anisotropy energy barrier of a single nanoparticle which means that it can help transferring heat under microgravity conditions if needed. However, aggregation among super-paramagnetic IONPs is a common phenomenon. Hence, for protecting

bare IONPs against aggregation, the magnetic properties can be tailored by the coating materials, such as Au, Ag and Co_3O_4 or by adding an aqueous solution such as Polyethylene glycol (PEG) to it during the synthesis process.

2.2.2 Fe_3O_4 Synthesis and Preparation Methods

Weng et al. (2018) prepared Fe_3O_4 nanoparticles by firstly, mixing 20 ml of KOH and KNO_3 solutions then stir them for 30 minutes. Secondly, 10 ml of FeSO_4 was added to the mixture drop-wise which resulted in a dark green solution. At last, the solution was heated to 90°C then kept for 4 hours in a water bath to prepare Fe_3O_4 gel solution.

2.2.2.1 Co-precipitation Preparation

Wu et al. (2011) synthesized Fe_3O_4 nanoparticles by co-precipitation method. $\text{Fe}(\text{OH})_3$ precipitate was washed several times with de-ionized water. Then FeCl_3 solution was obtained by $\text{Fe}(\text{OH})_3$ precipitate dissolution with hydrochloric acid. Then measured amount of $\text{FeSO}_4 \cdot 7\text{H}_2\text{O}$ was added, then the molar ratio of Fe^{3+} and Fe^{2+} in FeCl_3 solution was adjusted to 1.5:1. Under ultrasonic agitation, black precipitate was produced immediately by adding sodium hydroxide (NaOH). The principle reaction is:



Kulkarni et al. (2014) prepared Fe_3O_4 by co-precipitation method. Ferric Chloride (FeCl_3) was mixed with Ferrous Chloride (FeCl_2) with molar ratio of 2:1 in distilled water. The solution was then heated up to 50°C for 10 minutes. After that, ammonia was added to precipitate the solution. All these steps were processed under

continuous stirring. At the end a strong magnet was used to separate the NPs from the solution and were cleaned many times using distilled water.

2.2.2.2 Combustion Method

Kulkarni et al. (2014) used oxidant agent Ferric nitrate ($\text{Fe}(\text{NO}_3)_3$) alongside with glycine, ammonium nitrate and starch as fuel. Raw materials were weighed and then mixed using an agate mortar pestle. The mix was then grinded continuously. The mixture was poured into a pre-heated crucible at around 500°C and kept for 2 hours till all the leftovers were evaporated. Finally, a black colored powder was obtained and collected for further characterizations.

2.2.3 Fe_3O_4 Applications

Researchers in the past decade have been working on developing the synthesis of the magnetic IONPs for different purposes. Not only for its fundamental scientific interest but also for its many technological applications, such as targeted drug delivery, magnetic resonance imaging (MRI), electromagnetic interference shielding (EMI), magnetic hyperthermia and thermo-ablation, bio-separation, and bio-sensing (Wu et al., 2015).

2.3 Shape Memory Effect

Shape memory effect is the phenomenon to recover the original shape of a material only at the presence of a right stimulus such as heat, magnetic field, electric field, or water like the case in human hair and nails (Zhou & Huang, 2015). This has been observed in many different materials including metallic alloys and polymers (Huang et al., 2013). Shape memory effect is usually associated with metallic alloys,

such as copper-Aluminum-Nickel, Nickel-Titanium and Iron-Manganese-Silicon (Santo, 2016). Shape memory effect consists mainly of two different processes; programming process in which the material (polymer in our case) is deformed into a temporary shape. Second process is the recovery process when the material recovers its original shape. Material can be heated using one or more of the three heat transfer methods namely: conduction, convection and radiation. Heating the material above glass transition temperature T_g is required to trigger the shape recovery process. Below T_g the material, specifically polymer, is said to be glassy and harder because the movement of polymer segments is frozen compared to when it is above T_g where the material becomes rubbery and relatively more flexible which makes the rotation around these segments freer.

There are two different types of shape memory effect, one-way and two-way. In one-way shape memory effect, the permanent shape is recovered after heating. A temporary shape can only be obtained after mechanical deformation which indicates that thermal and mechanical conditions need to change in a memory cycle. On the other hand, two-way shape memory effect could occur by just heating and cooling in the presence or absence of an external load. The permanent shape is obtained when a certain stimulus is applied, but once that stimulus is removed, the material will reprogram itself and obtain the temporary shape again (Hager et al., 2015).

Figure 2 shows the comparison between one-way and two-way shape memory effect in materials.

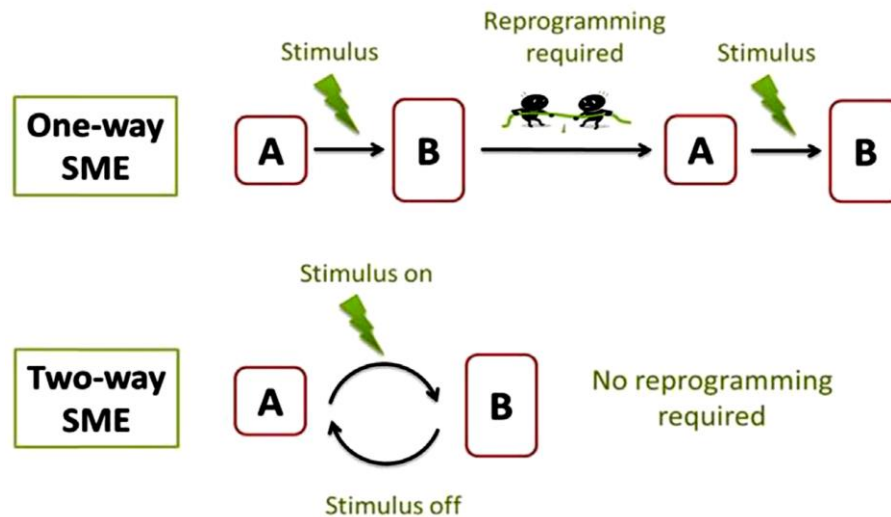


Figure 2: One-way VS Two-way SME

(Hager et al. 2015)

2.3.1 Shape Memory Polymers (SMPs)

Shape memory polymers (SMPs) are stimuli-responsive materials that have the capability of changing their shape upon application of an external stimulus. The stimulus is mostly heat, but light, electric and magnetic fields may also be used. Shape memory effect can be observed in heat-activated SMP when thermo-mechanical cycles are performed. These thermo-mechanical cycles consist of three main steps: firstly, the SMP is processed to its permanent shape. Secondly, it is heated up, deformed and then cooled down to receive its temporary shape.

Thirdly, it is heated up again to a certain temperature to recover its original permanent shape, in one-way Shape memory effect, any further cooling will cause the material to be stiffer and no further shape recovery can be observed. Steps are shown in Figure 3. SMPs usually contain at least two different types of segments or domains. The “permanent” segments or domains that determine the permanent shape are usually constructed from chemical or physical crosslinks. The “reversible”

segments or domains that determine the temporary shape are often formed at either the glass transition temperature (T_g) or the melting temperature (T_m). Upon increasing temperature, polymer segments get more freedom to move back to their thermodynamically favorable coiled structure to give maximum entropy.

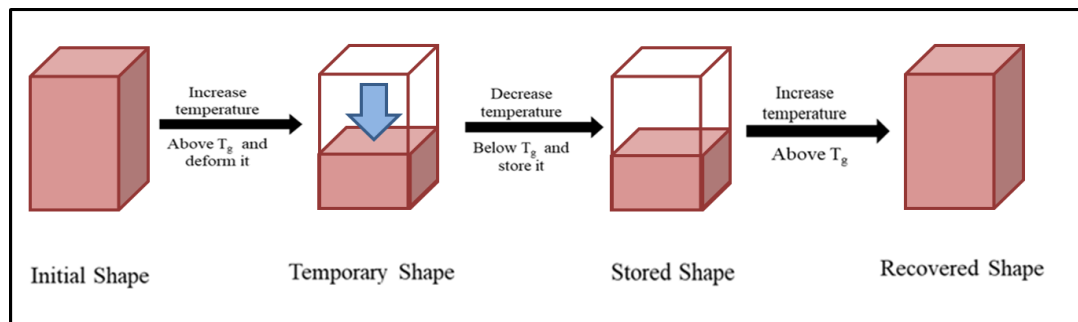


Figure 3: Shape memory effect steps in polymers

2.3.2 Shape Memory Foam

Polymers in foam structure have the advantages over the conventional structure for having lower density, more compressible, lighter weight, and lower recovery force with reduced stiffness and mechanical strength.

The common methods of producing polymer foams are complex as they require processing the polymer in liquid state. Foam can be produced by chemical or physical processes. In chemical foaming, a blowing agents are used to produce the foam, (Matuana et al., 2009) foamed Poly(lactic-acid) (PLA) with an endothermic chemical foaming agent (BIH40) through extrusion process.

On the other hand, a gas such as CO_2 is used in physical foaming process as a physical blowing agent and dissolved into the sample and then the gas is liberated. (Ito et al., 2014) studied epoxy resins (bisphenol/2-ethyl-4-methylimidazole) consisting of oligomers with different molecular weights and foamed it using a

temperature-quench physical foaming method with CO₂. It is also worth mentioning the work done by Dorigato et al. (2019) to foam cyclic olefin copolymer/exfoliated graphite nano-platelets using supercritical CO₂ treatment.

Yang et al. (2019) and his team managed to foam vinyl silicon rubber/CNTs/Fe₃O₄ nano-composite by batch foaming process using Sc-CO₂ at 70°C and 12 MPa for 2 hours and then the foamed samples were moved into an oven for 3 hours to further cure it. (Zhang et al., 2017) did a similar work when prepared PMMA nano-composite foam using CO₂ batch foaming. The system temperature was constant at 40°C and the pressure was 8.5 MPa for 16 hours to achieve saturation. They also released CO₂ and the samples were quickly immersed in hot oil at 110°C for 60 seconds and then used water at room temperature to stabilize the foams.

Ahmed et al. (2019) studied thermoplastic polyurethane/PLA blends foamed using supercritical CO₂ batch foaming and investigated the foamability of the sample by measuring the expansion ratio (which is the ratio of bulk density of the solid sample to the foamed sample) under a wide range of foaming temperatures (from 50 to 130°C) and CO₂ pressures (from 10 to 20 MPa). The foamed samples were prepared in a pressure vessel filled with CO₂ and were kept for 6 hours to allow CO₂ saturation then the pressure was released, and foamed samples were obtained. Results showed that a maximum expansion ratio was slightly more than 8 for the TPU80% sample at maximum CO₂ pressure of 20 MPa and maximum temperature of 130°C. The best foamability was shown by the TPU80% sample in which the cell size was almost 43 µm and lowest density at pressure of 10 MPa.

New developments are emerging in foaming process, the main purpose is to simplify the process and reduce the cost. Solid state foaming is a novel foaming method that does not require chemical reaction or physical foaming agent. (Quadrini & Squeo, 2008) used commercial epoxy resin to produce foam. The process starts by compact the epoxy powder into cylindrical tablets, different compaction parameters are verified such as packing pressure, packing rate and holding time, and an optimal one is identified. The compacted tablets are heated in a muffle at a temperature higher than the boiling point of the epoxy. Foaming temperature is constrained by the polymerization temperature as lower bound and the burning temperature as upper bound. The foaming time is found to be optimal at 10 minutes for samples used in the experiments. The foaming time is the minimum time required to reach full polymerization. Once the polymerization finishes the foam is left in still air to cool down to room temperature. Results showed that foam density decreased as packing rate, foaming temperature and packing pressure increased, while foaming ratio increased with packing rate, foaming pressure and packing pressure. The authors studied different process parameters and optimal parameters were determined.

Solid state foaming can be used to produce foams that exhibit shape memory effect. Fabrizio et al. (2012) investigated the physical and mechanical properties of a shape memory foam produced using solid state foaming process. The objective of the study was to maximize the actuation load, the load which the foam exerts during shape recovery. Three different tests: compression, flexure and torsion were carried out. Actuation load was assed firstly during the compression test; the sample started to push at a temperature about 100°C then a sudden increase of the actuation load was observed at 120°C to a maximum of 6.3 N. Flexural test showed that the actuation load started at lower temperature of 80°C, with a maximum load of 5.31 N

observed at 120°C. The torsion test showed low actuation load of 0.32 N. It is obvious that the maximum actuation load is different from one configuration to another; this could lead to investigate if the foam has directional mechanical properties, and no explanation was given by the authors. The study also did not provide explanation of the achieved recovery ratios.

Yao et al. (2018) prepared cross-linked PCL/silk fibrin (SF) composites and foamed it using solid state foaming method. They dissolved series of PCL into dichloromethane with different Benzoyl peroxide concentrations, and then SF was dissolved into PCL/BPO. The mixture was then dried at room temperature under air atmosphere resulting in creation of PCL films. These films were then cut into specific size and placed into a suitable mold. These pieces were then compacted and cured at 80°C for 3 hours in an oven to produce the foam. Maximum pores density was almost 2500 cm³ at lowest BPO concentration of 5wt%.

2.3.3 Shape Memory Polymer Composites

Shape memory composites are said to have higher strength, higher stiffness and special properties determined by the type of fillers that are added, which can offer further advantages over SMPs. However, shape memory composite foam has relatively low actuation load, even if one tried to improve the stiffness and increase the actuation load, the foaming process will usually be negatively affected by the addition of fillers (Santo et al., 2012).

Abdullah & Ansari (2015) studied the effect of different volume percentage of Graphene Oxide (GO) (1.5, 3.0, 4.5 and 6.0 vol%) on epoxy resin. The results showed increment in tensile strength after the addition of GO with maximum tensile

stress of 13 MPa @1.5 vol%. The more GO added to the matrix the more increment observed in Young's modulus to maximum value of 206 MPa. Same thing can be said about the elongation as it increased with more GO vol% introduced to the matrix.

In another study done by Zheng et al. (2009), the authors prepared poly(d,l-lactide)/Fe₃O₄ composites at different weight ratios. They concluded that the more Fe₃O₄ content introduced to PDLLA matrix caused the tensile strength of the composite to increase almost by a factor of 1.5 compared to pure PDLLA. Fe₃O₄ presence also resulted in some holes in the polymer matrix due to discontinuity in the matrix.

The mechanical properties of PCLAU/Fe₃O₄ nano-composites studied by Gu et al. (2018), showed decrement in yield elongation and break elongation as Fe₃O₄ content increased. On the other hand, yield strength increased to maximum value of 20 MPa at 6 wt% of Fe₃O₄ and elastic moduli increased from 426 to 743 MPa also at 6 wt% of Fe₃O₄, further increment in Fe₃O₄ caused it to aggregate and had a negative impact on mechanical properties. The shape memory effect was triggered via heating and it showed a great recovery ratio to a value up to 86.46% at 40°C and 9 wt% of Fe₃O₄. The shape memory properties improved as content of Fe₃O₄ increased.

Soto et al. (2018) prepared polyurethane/Fe₃O₄ composite by a simple suspension casting method and studied the effect of different wt% content of Fe₃O₄ on different properties of the composite. Results showed that the addition of magnetic NPs did not significantly affect the shape memory behavior or other mechanical properties. However, it added magnetic response to the nanocomposites. Thus, nanocomposites were able to increase in temperature to higher temperature than the

melting point of PU soft segments in about 10 seconds when exposed to an alternating magnetic field of 260 kHz frequency and 48 kA/m magnetic field density, which allowed them to recover their original shape quickly (less than 30 seconds) by an indirect triggering method.

Vialle et al. (2009) selected Thermoset epoxy (DP5.1) shape memory polymer resin and filled it with Fe_3O_4 NPs of different amounts varying from 2.5 to 10 wt%. They mixed the matrix and the nanoparticles then foamed it to get a high level of dispersion. Results showed that the filler content has little effect on the compressive response of the foams as well as no significant effect on the externally thermally activated shape recovery. A fastest shape recovery was observed at 10 wt% of MNPs (17 seconds) where shape recovery rate has increased when the temperature crossed T_g of the epoxy resin. The authors however did not show the shape recovery percentage of the foam samples.

Squeo et al. (2010) investigated the effect of adding Nano-clay particles to shape memory foam produced by (Quadrini & Squeo, 2008). Percentages of 0, 1, 2 and 5 % were investigated; the effects on the foaming ratio, microstructure, transition glass temperature, dynamic mechanical behavior, and compressive toughness were verified. The study concluded that foaming ratio decreases by increasing the filler percentage, while the toughness shows opposite behavior. The data confirmed decrement in the glass transition temperature with the filler content increases. Results confirm the strong influence of the filler content on the molecular mobility of foam samples, this leads to the fact that a large increase of the storage modulus is obtained by increasing the filler content. Although the compressive toughness was improved by the addition of the nano-clay, yet the foaming ratio linearly decreased because the

foam dissipates the energy by flattening pores. The energy per unit volume increased with increasing the MMT wt%. Not only that, but also the energy per unit mass increased as well with increasing the content of MMT.

Weng et al. (2018) managed to prepare PI/Fe₃O₄ nano-composites with different Fe₃O₄ content introduced to PI matrix (from 0 to 13 wt%) and foamed it. They tested different properties of the foam starting from morphological, dynamic thermal behavior, density measurements and compression properties. The observed thermal degradation temperature showed increment as Fe₃O₄ content increased from 300.2°C to 301.4°C whereas the T_g has dropped to 314°C compared to 336°C for pure PI and this is due to the discontinuous inorganic phase caused by the NPs. For mechanical properties, as Fe₃O₄ content increased, impact strength dropped down to 0.0491 kJ/m², compressive strength increased to maximum of 0.31 MPa and the foam density increased up to 26.8 kg/m³. The author however did not specify the definition of foam density and how it was calculated.

2.4 Applications of Shape Memory Polymers

Potential applications for SMPs occur in different fields, including Aerospace industry, Radar absorbing, Fire-proof materials, Oil absorbents, switches and sensors. They can be used also for heat shrinkable tubes; auto repairing and self-healing (Kausar, 2018). Open-cell shape memory polymer foams also showed good potential to be used in automotive seats as it decreases the total weight. Fiber-reinforced polymer foam was used to construct an automotive panel system as well as sound absorption material due to their excellent acoustic properties.

Other potential applications are in the biomedical field: drug delivery, biosensor, biomedical devices. Moreover, since polymer can be made biodegradable, they can be used as short term implants where removal by surgery can be avoided (Ratna et al., 2008).

Shape memory polymer foams can be also used in intracranial aneurysms treatment as done by Wang et al. (2019), they developed SMP foam using sugar template method and infiltrated CNTs into the matrix via ultrasonication method, they used the SMPF in this specific application because of its low density, high porosity and excellent compressibility compared to the conventional materials used such as microsurgical clipping and endovascular coil embolization.

Shape memory polymer foam can also be a good contributor for materials in electromagnetic shielding field. This field is quite important because of the increase usage of EM devices such as wireless networks and communication equipment. Weng et al. (2018) prepared polyimide/ Fe_3O_4 nano-composite foams and showed that these foams exhibited excellent super-paramagnetic and thermal properties which gave potential promises in EMI field. PI is a good candidate in this field due to its special properties most importantly high radiation and chemical resistances, in addition to low thermal conductivity. If that is added to the excellent magnetic properties of Fe_3O_4 then the result will be a great composite for EM shielding.

Shape memory polymers are very useful for microsystem components, smart textile and in aerospace for actuators and self-deployable structures (Ratna et al., 2008). The main advantages of these actuators are the system simplicity and the low displacement rate (Santo, Tedde, & Quadrini, 2015). Another possible application

could be the fine regulation of the position of shields, mirror, and other structures for satellites (Santo, 2016).

In space applications heat transfer within the foam matrix is not as efficient as it is under macro-gravity conditions and the reason is that foam itself is not a thermal conductor (Santo, 2014). To resolve this issue, it is suggested to add filler that can be activated remotely by an external stimulus to transfer heat. Soto et al. (2018) studied the ability of Fe_3O_4 magnetic NPs to increase PU matrix temperature and found out that the more MNPs content it is, the higher the final temperature achieved.

2.5 Critical Review

Shape memory materials have been extensively studied and tested, by researchers, to evaluate their possible applications. This is especially true of shape memory polymers and foams. The foamed structures have many attractive properties such as low density, light weight, and the ability to be compressed and recover their shape. However, these foamed polymer structures have not been studied in great details when foamed using solid state foaming process, Hitherto, this process has been used to generate metallic foams, but is still a relatively new process in the field of polymer foams. This research aims to study the possible applications of this novel foaming process on epoxy polymer powders and how different factors might impact on the foamed sample produced and its performance. It will also consider how these controlled factors can be manipulated to obtain the best foam structure and performance.

Chapter 3: Experimental Methods

This chapter describes the methodology employed to prepare and characterize the polymer tablets, nanoparticles and nano-composites under a series of differing conditions. Specific details of the experiments and machinery used will also be described in detail.

3.1 Sample Preparation

3.1.1 Nanoparticles Preparation

The first step was to prepare the nanoparticles by using a co-precipitation method. In this method, ferric chloride and ferrous chloride are mixed in a ratio of 2:1. These Fe^{2+} and Fe^{3+} solutions are prepared by creating an aqueous solution in distilled water. The solution, containing both ions, is then heated to 50°C for 10 minutes. After heating, the solution is precipitated via ammonia solution which is continuously stirred using a magnetic stirrer at a 50°C temperature. As a result, black-colored iron oxide particles are produced and are then separated from the solution by a strong magnet before they are cleaned with distilled water. The resultant powder is then slowly air-dried.

3.1.1.1 X-ray Diffraction (XRD)

To ascertain structural properties, X-ray diffraction (XRD) was performed to characterize the prepared nano particles. The test was conducted using copper $\text{Cu-K}\alpha$ radiation with a wavelength of $\lambda = 1.540 \text{ \AA}$, at a scanning rate of 2° per minute within a range of 20° to 80° . Figure 4 shows the XRD pattern for the Fe_3O_4 . The pattern matches perfectly with the standard patterns shown in Figure 5 where the

prepared and standard Fe_3O_4 was compared. Estimating the crystal size of the nanoparticles was achieved by using OriginPro8 software and the Sherrer's equation below:

$$D = \frac{K \lambda}{\beta \cos \theta}$$

Where D is the crystal size, K is Sherrer's constant and it is equal to 0.9, λ is the source wavelength and it is equal to 0.1540 nm and β is the full width at half maximum (FWHM) and θ is the peak position on x-axis. The average crystal size was 9.71 nm for the prepared NPs.

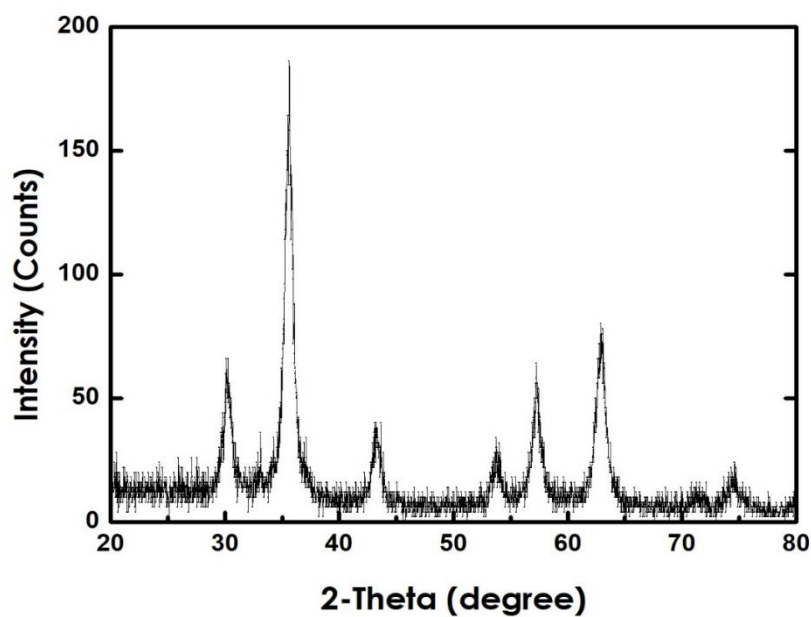


Figure 4: XRD pattern of the prepared nanoparticles

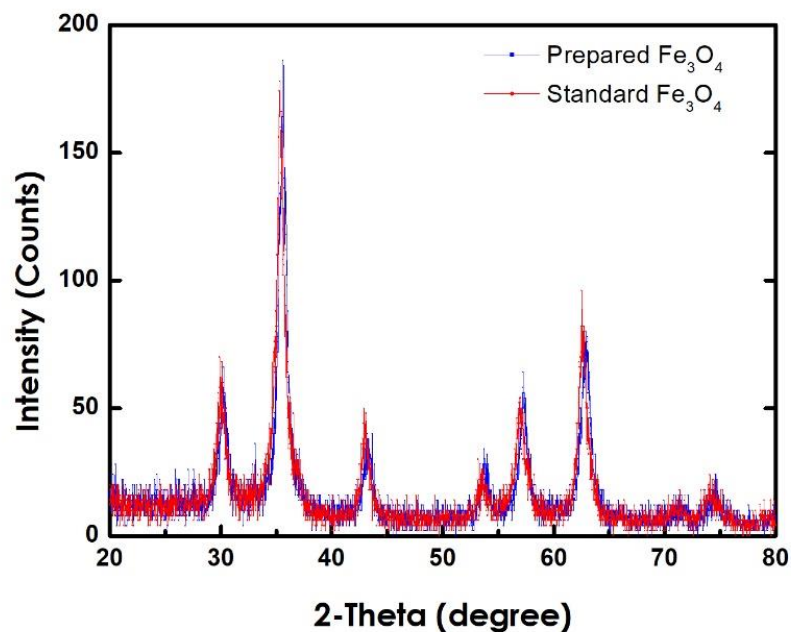


Figure 5: Comparison between the prepared and the standard Fe₃O₄

3.1.2 Selection of Polymers

The polymers chosen for this research were polyester-based polymers; which get excited and break their inter-polymer bonding when exposed to enough heat. These bonds reform when the structure is cooled down. This feature makes polyester based polymers suitable for this research, where melting and then foaming is required.

First polymer used was Corro-Coat PE Series 7 purchased from Jotun paints. This is a polymer usually used to paint fixtures and automotive parts and accessories. What make this polymer of a great potential for this study, is its reactive carboxyl groups, and the fact that it is cured by Triglycidyl Isocyanurate (TGIC). TGIC has three pendant epoxide groups that react with the carboxyl groups on the polyester resin in an additive fashion, and so serves our purposes as it acts as a crosslinker.

Second polymer, namely Jotun Super Durable 2903 is a TGIC free powder with no volatile organic compounds which makes it eco-friendly product, its main applications are in claddings and coating of architectural extruded aluminum. Both polymers exhibit semi-crystalline behavior, meaning they consist of crystalline regions separated by amorphous regions, which creates an opportunity for filler diffusion (Fe_3O_4 NPs, in our case) throughout the amorphous regions.

3.1.2.1 Functional Group Analysis

Fourier Transformation infrared (FTIR) was carried out with both polymers in order to conduct a functional group analysis. During the investigation, different absorption bands were detected on pure PE, most importantly a strong band at 1750 cm^{-1} which indicated C=O stretching. The occurrence of this band proves the existence of ester functional group in the polymer. Additionally, medium bands at 1950 and 1550 cm^{-1} indicated C=O=C stretching and N-O stretching, respectively. Proof of the existence of TGIC is found in the C-N peak at around 1450 cm^{-1} as shown in Figure 6.

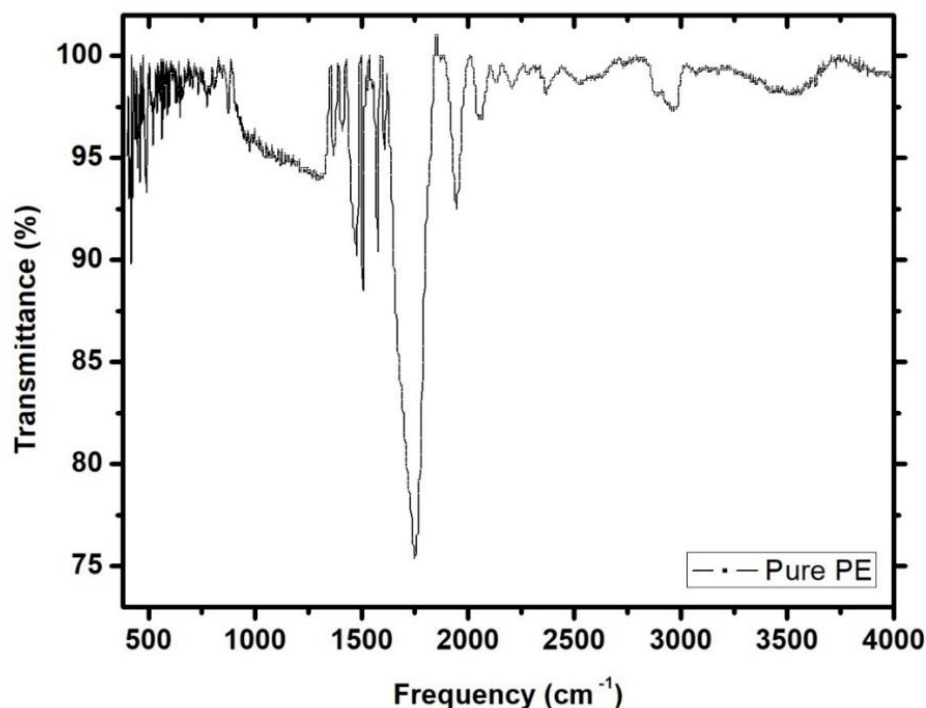


Figure 6: FTIR bands of pure PE sample

3.2 Design of Experiment

After nanoparticles preparation and selection of the polymers, a thorough investigation was conducted to determine the influencing factors in the solid-state foaming process; six factors were found to be the most critical ones, Figure 7 exhibits these factors. One factor at a time approach was followed to determine the best levels (working range) of each factor. Two levels of each factors were determined. The research objectives, see section 1.4, are optimizing the foaming process as well as the shape memory effect. These objectives were translated into the following outputs:

A. Foaming process:

1. Foaming ratio

B. Shape memory effect:

1. Actuation load
2. Shape recovery speed

Large number of experiments is required to study the effect of the six factors on the above output, mainly, $(2)^6 = 64$ experiments are needed. Taguchi design of experiment is statistically and imperially approved approach to reduce number of essential experiments required to study the effect of N factors with L levels on a specific output. The main principle behind Taguchi design is to use specially designed orthogonal arrays to study the effect of certain number of parameters while using only a comparatively small number of experiments to examine the main factors affecting the output. Minitab software can be used to generate Taguchi design of the required experiments. The formula below showing the minimum number of experiments as formulated by the Taguchi design.

$$N_{Taguchi} = 1 + N_v (L - 1)$$

Where:

$N_{Taguchi}$ is number of experiments to be conducted,

N_v Is number of parameters and

L is number of levels for each parameter.

In this research, six (6) different factors were selected in order to study their effect on the foaming process. These variable factors were as following: the percentage of NPs, type of polymer, packing pressure, holding time, foaming temperature and foaming time spent in the oven. The different process parameters and responses are shown in Figure 7.

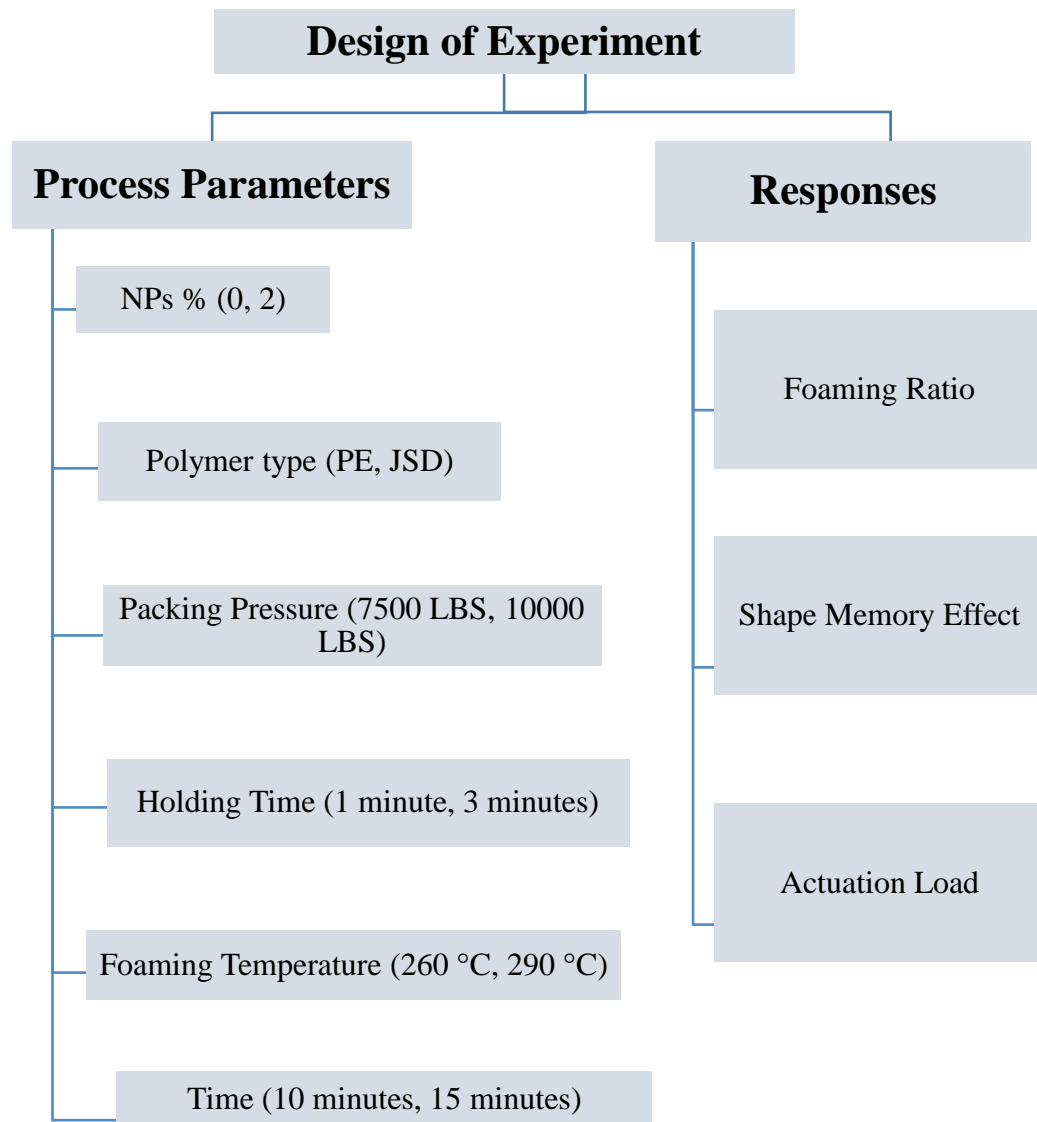


Figure 7: Process parameters and Responses

Two levels were chosen for each parameter, starting with 0 and 2 NPs percentage, corro-coat PE series 7007 (henceforth referred to as PE) and Jotun Super Durable 2903 (henceforth referred to as JSD) polymer types. 7500 and 10000 LBS packing pressures, 1 and 3 minutes holding the sample under the packing pressure. 260 and 290°C foaming temperatures and lastly 10- and 15-minutes foaming time. The total number of experiments required under the Taguchi formula was seven. However, in order to incorporate the balancing property of the orthogonal arrays, the

total number of experiments in our case reached eight. The total number of experiments shall be multiple of 2 or 3. The orthogonal array design for this research can be found in Table 1: Taguchi map designed for this research below. Three replicas were performed for every run, this is to minimize the effect of uncontrolled factor such as random error.

Table 1: Taguchi map designed for this research

Parameters Run #	NPs%	Polymer type	Packing Pressure (LBS)	Holding time (minutes)	Temperature (°C)	Foaming Time (minutes)
1	0	PE	7500	1	260	15
2	0	PE	7500	3	290	10
3	0	JSD	10000	1	260	10
4	0	JSD	10000	3	290	15
5	2	PE	10000	1	290	15
6	2	PE	10000	3	260	10
7	2	JSD	7500	1	290	10
8	2	JSD	7500	3	260	15

3.3 Foaming Process Procedures

Solid state foaming process uses compacted powder in a form of tablet. These tablets were placed in a mold, and then heated up in an oven to a temperature enough to melt the tablet and boil the melt. Samples were removed from the oven and left in the still air to cool. The final structure is a solid with pores; this form is the foamed shape of the polymer. Below are the detailed steps of foaming process followed in this research.

Step 1: Preparation of the Tablet

After designing Taguchi Map, it was the time to prepare the tablets to be foamed. The tablets prepared here exhibited different parameters, as based on the Taguchi Map. The tablets for the first two runs were for PE with 0% NPs packed under 7500 LBS packing pressure exerted by a hydraulic press machine. One was kept under pressure for 1 minute, while the other was kept under the same pressure for 3 minutes.

For run numbers three and four, the JSD polymer was mixed with 0% NPs, and packed under 10000 LBS of packing pressure. Once again, the holding time differed from 1 minute for run three, and 3 minutes for run four. The tablets in runs five and six were prepared using PE mixed with 2% Fe_3O_4 NPs under a packing pressure of 10000 LBS. Similarly, run five was held under pressure for 1 minute, whereas run six was kept under pressure for 3 minutes.

The final two runs used a JSD polymer with 2% NPs. This mixture was pressurized by a hydraulic press under a packing pressure of 7500 LBS for 1 and 3 minutes, respectively. Mixing the polymer powder and Fe_3O_4 NPs was achieved by pouring them into a test tube and shaking by hand until the color changed.

In every experiment a tablet of total weight of 5 grams is produced, the 5 grams were the total of the powder and the NP addition. In cases of tablets without NP, then the 5 grams are pure polymer powder. Polymer powder and Fe_3O_4 NPs, was poured into a stainless-steel mold with an inner diameter of 20.3 mm and was then packed gently into the mold using a stainless-steel plunger. Tight mold-plunger assembly clearance (0.15 mm) was selected to avoid any powder loss when packed by a

plunger. The whole setup (the mold, plunger and powder) was placed on a stainless-steel base to keep the powder from sticking to the machine's surface (see Figure 8).

A Carver Hydraulic Press System was used to provide the required pressure at a pump speed of 30% (1.56 mm/sec). Applying high pressure to the powder caused it to stick together and form a tablet with the desired dimensions – almost 9 mm in height and 20.3 mm in diameter. Finally, a tablet was extracted from the mold with gentle hammering to avoid cracking or breaking the tablet.

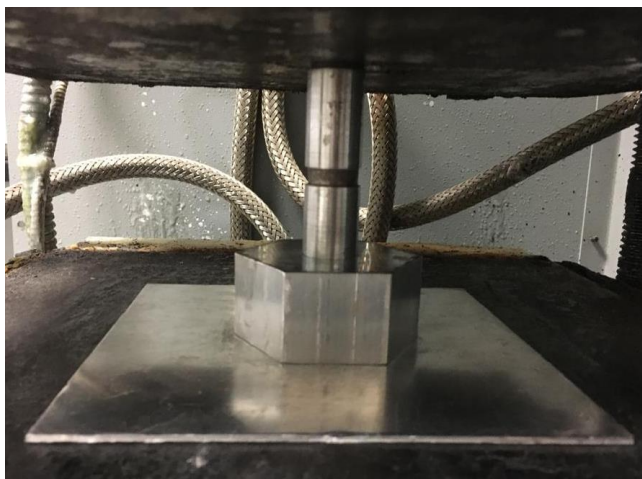


Figure 8: Stainless steel mold containing the powder that is to be packed using the hydraulic press machine

Step 2: Tablet foaming

After the tablet was extracted, it was ready to move to second processing stage, namely the foaming stage. Prior to foaming the tablets, foaming temperature and the foaming time had to be determined. Thus, a pre-test was carried out to study the best foaming temperatures. More details about the test will be discussed later, in optimizing foaming process chapter.

According to our original Taguchi Map, tablets from first and sixth experiments were all PE polymer and its mixture with 2% NPs foamed at 260°C and kept inside the oven for 10 and 15 minutes respectively. JSD polymer and mixtures with Fe₃O₄ NPs, were formed (as tablets) from experiments three and eight. In both experiments, the foaming temperature was set to 260°C and they were again kept inside the oven for 10 and 15 minutes, respectively. On the other hand, tablets obtained from experiments two, seven, four and five were foamed at a temperature of 290°C, with a foaming time of 10 minutes for experiments two and seven. Whereas experiments four and five were kept inside the oven for 15 minutes.

All the tablets were placed on a thick aluminum sheet and then slowly inserted inside another mold (see Figure 9 and Figure 10) with an inner diameter of 20.7 mm. They were then placed in an oven set to a predetermined temperature to cause the foaming process. These tablets were placed in the oven for specified times and were allowed to cool in still air for 15 minutes. The resultant sample shape was cylindrical. This used foaming technique is called solid-state foaming and it was proposed and tested for the first time on polymers using 3M epoxy resin (Quadrini & Squeo, 2008). Other foaming techniques are detailed in the literature and background chapters of this thesis. After foaming, the samples were extracted from the mold and were then transferred for further testing.

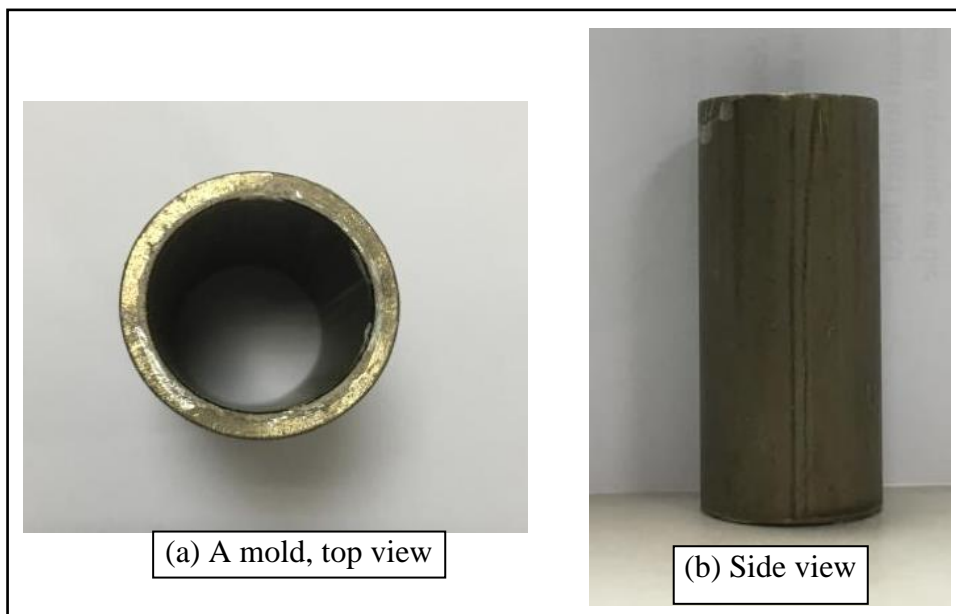


Figure 9: A mold used to insert the sample inside the furnace for foaming process

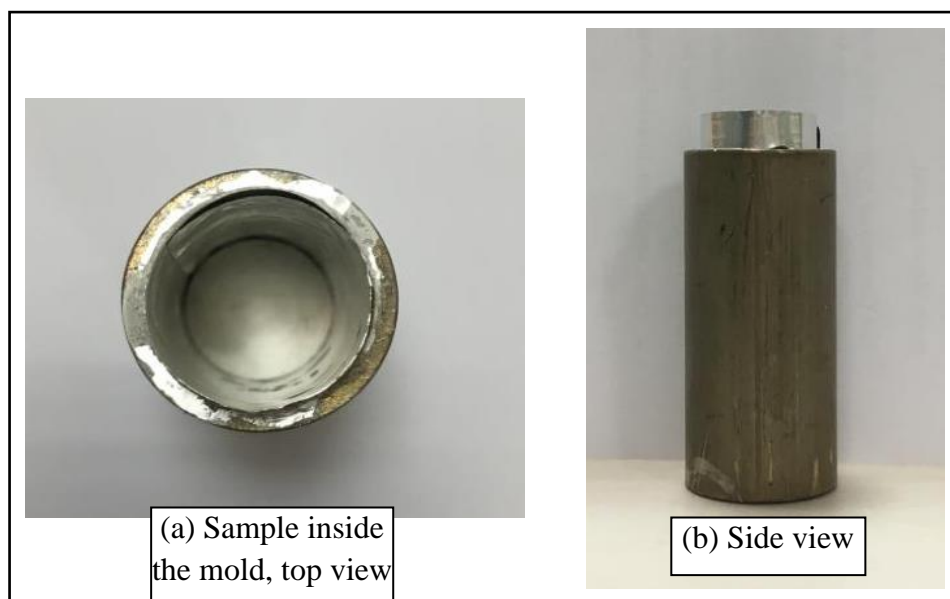


Figure 10: Prepared tablet inserted inside a thick aluminum sheet and a mold on a stainless-steel base ready to be foamed

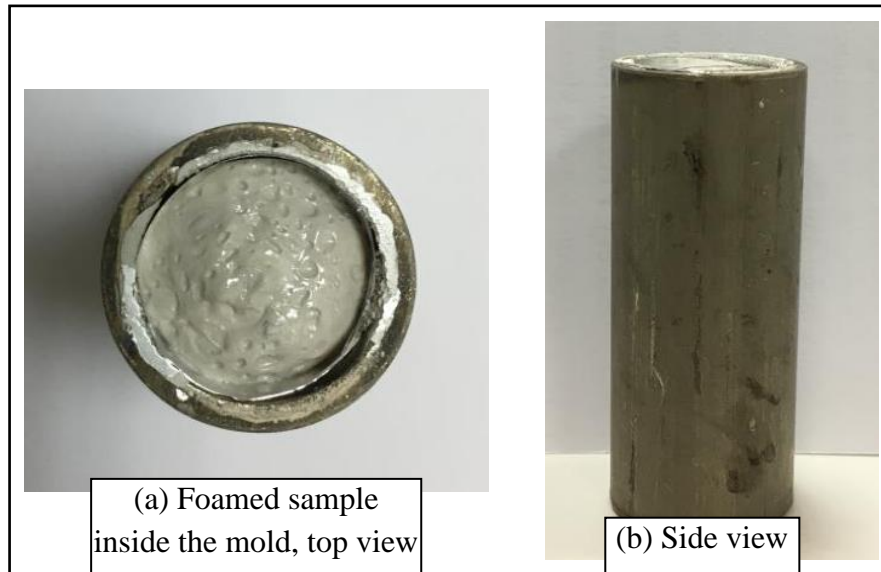


Figure 11: A Samples after the foaming process and removal from the oven, ready to be extracted from the molds

Step 3: Sample machining

It was necessary to remove the aluminum foil, used in the foaming process, in order to obtain the samples, refer to Figure 11. These foamed samples did not have regular dimensions, especially on the upper part, where they tended to form either a dome shape or left some void in the middle and formed higher foam on the sides of the cylinder mold. These deformations occurred because solid state foaming is considered as an uncontrolled process, so it was necessary to machine them into a regular shape with uniformed heights for easier calculations as shown in Figure 12. After achieving a uniform height and length, the foamed samples were ready for testing.



Figure 12: Samples being machined and shaped into a uniformed shape for easier calculations using a CNC machine

3.4 Measurements

3.4.1 Foaming Ratio

Foaming ratio measurements were performed on three replicas from each experiment. The foaming ratio in this research is defined as the ratio between the foam height and tablet height. The height and diameter of each sample was measured to obtain values for volume after it was air-cooled, a digital caliper was used for this regard. The mass was also measured using a single pan analytical digital balance. This is conducted for the three replicas in every sample in each run. The average of these replicas is recorded as the final value for the foaming ratio associated with that run. All data was entered into an excel sheet which used the formula below to calculate the volume of a sample

$$V = \pi r^2 h$$

Where V is volume of the sample, r is radius of the sample, and h is the height of the sample.

After the volume was calculated, then the foam density of each sample can be calculated by dividing the sample average mass by the calculated average volume. Foaming ratio and density of a sample has inversely proportional relationship. Higher foaming ratio leads to lower density. This relationship is applicable in case of pure polymers, but not necessarily applicable in case of polymer with NPs.

3.4.2 Shape Memory Effect

Samples of three replicas were prepared to test the shape memory effect. Same technique as above was followed. All the foamed samples prepared from each set of experiments were placed in an oven previously heated to 120°C. They were kept at that temperature for 2 minutes to soften their structure and make it easier to compress them.

Subsequently, these samples were compressed for 1 minute under room temperature in an air environment to 50% of their original height using a plunger and placed inside a cylindrical mold in order to direct the motion of the sample during the compression, then they were allowed to cool to reach their temporary shapes.

After that, the samples were placed inside the oven once again to allow for shape recovery. The samples were removed once they had returned to their original height, with a high recovery ratio of 95% (see Figure 13).

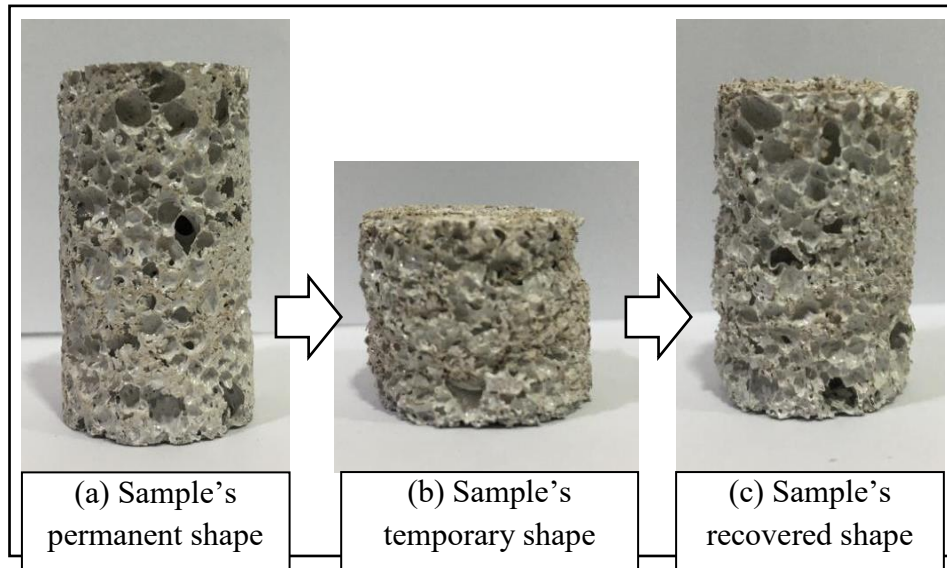


Figure 13: A sample just heated, compressed to 50%, recovered its original height

The Recovery time is recorded starting the moment the sample start the recovery till it reaches its final height. Samples started recovery once the temperature inside the oven reached 120°C. Recovery speed was calculated by dividing the distance recovered by the recorded recovery time.

3.4.3 Actuation Load

A new set of three samples from each experiment was prepared for this test. The samples were placed inside an oven for 2 minutes at 120°C to soften their structure, and then the samples were compressed to 50% of their original height using a plunger to place them inside a cylindrical mold. The samples were then allowed to cool down in an air environment for 5 minutes to achieve their temporary shape.

After that, the samples were placed in an oven and were put in slight contact with a digital force gauge (DFG35 Digital Force Gauges) especially prepared for this test. Subsequently, the force gauge was moved upwards to make 0.0 N contact force

with the compressed sample (refer to Figure 14 for a sample graph from the force gauge data).

The temperature inside the oven was then increased to 120°C and the samples were kept at that temperature for 1 minute to allow for shape recovery. The temperature was then gradually decreased to room temperature. The force gauge readings were obtained using MESUR Lite software to determine the actuation load.

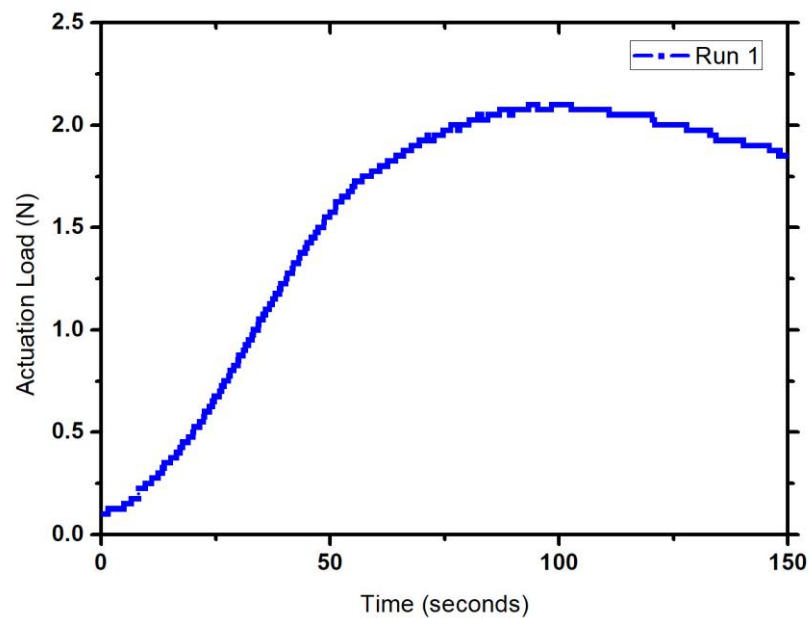


Figure 14: A graph generated using data extracted from MESUR Life software and the force gauge

3.4.4 Optimum Processing Parameters

Optimum parameters were selected prior to all tests and results obtained, this test suggests the best levels needed to be used in order to get the highest possible optimum value for all properties involved namely: foaming ratio, foam density, recovery speed and actuation load. It is expected not to get the optimum value in all

tests as not all properties give best results under same levels and conditions, Therefore, this test chose the optimum value for each level to get the most suitable outcome for each property. Nine (9) samples were prepared for each of the selected levels to obtain an accurate average value for each property.

3.5 Sample Characterization

Sample Characterization is an essential step in obtaining data and analyzing it for better understanding of its behavior. In our case, different characterization techniques were carried out on the two polymers (PE and JSD) in their powder form and on our nanoparticles.

Differential Scanning Calorimetry (DSC) is a technique used to measure glass transition temperature. A reference sample was used to achieve greater accuracy and a better understanding of the behavior of the characterized sample. The machine used in this research operated in a temperature range from 30°C to 250°C with an accuracy level of up to $\pm 0.1^\circ\text{C}$. All the samples were heated from room temperature up to 250°C at an incremental rate of 10°C/minute to remove heating history in the sample. Then it was cooled at the same rate back to room temperature. Finally, the samples were heated up again to 250°C at a rate of 10°C/minute. DSC was operated on pure PE polymer, PE+0.5 w.t% Fe_3O_4 , pure JSD and JSD+2 w.t% Fe_3O_4 NPs. The samples' measured weight was 8.3 mg, 6.8 mg, 8.1 mg and 8.2 mg respectively.

The Fourier Transformation Infrared Spectroscopy (FTIR) technique is used to identify and investigate the chemical composition of the polymer and to determine the functional groups in the sample. It depends on the vibration/rotation of the bonds in the molecules. Once an infrared spectrum is emitted, the sample absorbs some

radiation at certain frequency depending on the vibration and rotation modes of these bonds. This test was carried out on Pure PE and JSD powders.

X-ray Diffraction (XRD) was used to determine the crystal size apparent in our nanoparticles. The basic principle of this machine depends on the diffracted x-rays from the sample's plane following Bragg's law. The machine examined Fe_3O_4 nanoparticles within an angle range of 20° to 80° at a scanning rate of $2^\circ/\text{minute}$. The machine used a $\text{Cu-K}\alpha$ x-ray source. The graphs obtained from the XRD machine were analyzed to determine the crystal size of the sample using a Sherrer equation.

Chapter 4: Optimizing Foaming Process

The foaming process is a critical step when producing samples to be studied. This chapter is concerned with the process model, determining process parameters, the results of foaming ratio measurements, an analysis of the results, as well as a configuration of the selected levels based on the results and analysis

4.1 Process Model

A process model is a common starting step when designing experiments. The model includes input (polymer type and NP% in our case) into the process, the controlled factors that can be manipulated and changed by the researcher, the uncontrolled factors that researchers cannot change or control, and finally, the output of the process – namely foaming ratio and density, shape recovery speed and actuation load. The process model for this study can be seen in Figure 15.

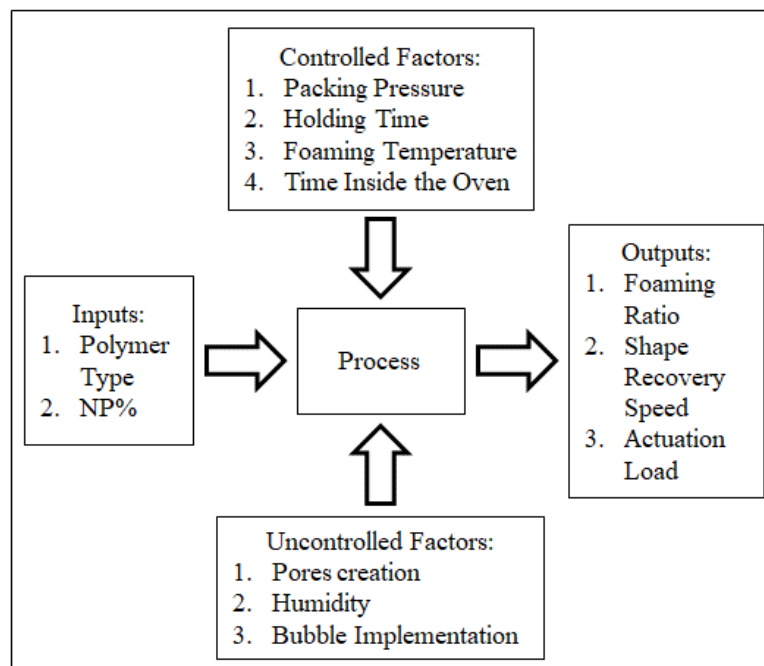


Figure 15: Process model of this research

4.2 Process Parameters

Before proceeding with the experiments, one needs to define and set the process parameters that can affect the process. The factors in this research are polymer type, NP%, packing pressure, holding time, foaming temperature and foaming time. Each of these factors has different levels determined through pretesting. This will be discussed in more detail in this section.

4.2.1 The Determination of Foaming Temperature

Samples prepared were pure PE and PE+2 w.t% Fe₃O₄ NPs, as well as pure JSD and JSD+2 w.t% Fe₃O₄ NPs. The main goal of this experiment was to test the best foaming temperature. Foaming temperatures tested were 200, 240, 260 and 290°C, the selection of these values was not random as it had to be optimized to avoid burning and assure polymerization of the polymer powder. The temperature at which the lowest density obtained is considered as the best foaming temperature. Results perfectly match with (Quadrini & Squeo, 2008). It is clear from Figure 16 and Figure 17 that increment in the foaming temperature causes an increment in the foaming ratio, which results in larger pores within the both polymers' matrices. Foaming temperature impact on PE polymer was maximized between 260°C and 290°C but the difference between these values were not significant. On the other hand, JSD showed different range of working temperature at which highest foam ratio is obtained. However, 260 and 290°C were selected to be the 2 levels for the foaming temperature factor because of their obvious positive impact on the ratio of PE foam.

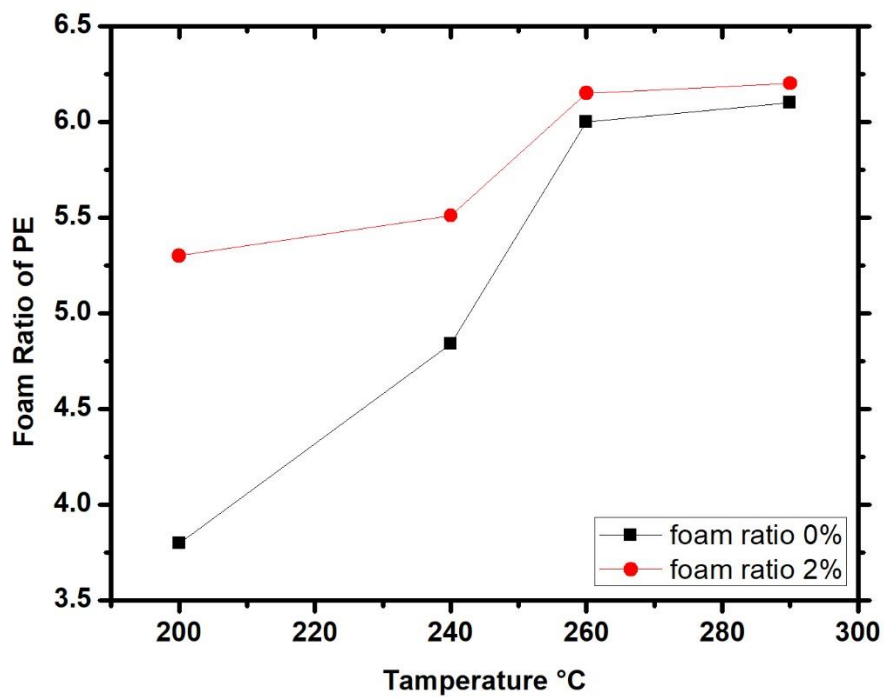


Figure 16: Foam ratios as a function of temperature for pure PE and PE+2% NPs

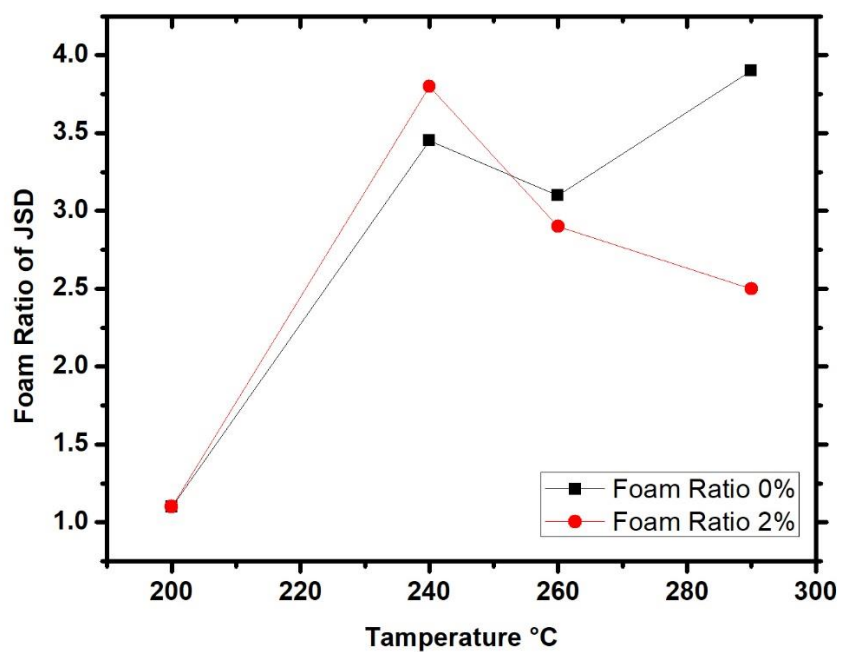


Figure 17: Foam ratios as a function of temperature for pure JSD and JSD+2% NPs

4.2.2 Nanoparticles Percentage

The addition of nanoparticles can have different impacts based on the percentage present in the polymer matrix. A pretest was carried out on the effect of Fe_3O_4 NPs on the speed of shape recovery in the PE matrix. The results are shown in Figure 28. Results showed that a further increase in the NP% to a value more than 2% will have a negative impact on shape recovery speed in the PE tablets. Thus, it was decided to select 0% and 2% additions of NPs as part of the total weight of the tablets.

4.2.3 Packing Pressure

Exerting packing pressure on the powder is important in order to ensure the creation of well-packed tablets that can be foamed later. A pretest was carried out to study the effect of packing pressure on the foam ratio of the PE tablets. We found the optimum values for a good foaming ratio under pressure from the hydraulic press machine were 7,500 and 10,000 lbs., respectively. Because any further decrement will not allow the tablet to foam in a regular manner as shown in Figure 18. Therefore, these values were chosen for packing pressure.



Figure 18: Irregular sample foamed at 0 LBS packing pressure

4.2.4 Holding Time

The time the polymer powder is kept under continuous pressure is the least effective factor according to the Taguchi analysis of the sample. We saw that its effect was minimal on the foaming ratio and density, shape recovery speed and actuation loads. Thus, the levels selected were limited to the performance of the machine between 1 and 3 minutes.

4.2.5 Foaming Time

The exposure of the tablet to temperature is an important factor that impacts both the foaming ratio and density measurements. Different foaming times were selected and tested to determine optimum levels. JSD and PE tablets were prepared for foaming in the oven for 5, 10 and 15 minutes. Samples foamed at 5 minutes did not have enough time to generate pores within their structure and thus the foaming ratio measurement was not available for study. However, both the 10- and 15-minute foaming periods showed significant results for both polymer tablets and thus they were the selected times. Further increment in foaming time is not advisable as it will cause a burn in the polymer.

4.3 Foaming Ratio and Density Measurements

The foaming ratio is defined as the ratio between foam height and initial tablet height. These heights were measured using a digital caliper to ensure accuracy. The density was calculated using the formula below:

$$\rho = \frac{m}{V}$$

Where ρ is the density of the foam, m is the mass of the foamed sample, and V is the measured volume of the foamed sample.

Prior to the Taguchi Map design and selecting the foaming temperature levels, three samples were prepared from every set of experiments to determine the best parameters in order to obtain the highest foaming ratio and the lowest foam density. Average foaming ratios and densities were calculated using excel software for each experiment. The results were later analyzed using Minitab software. The respective foaming ratios and densities can be found in Table 2.

Table 2: Average calculated foaming ratio and average foam density for each set of experiment

Run #	1	2	3	4	5	6	7	8
Average Foaming Ratio	5.43	5.54	3.18	3.96	6.21	5.79	2.56	2.96
Average Foam Density (g/cm ³)	0.25	0.23	0.31	0.28	0.21	0.20	0.37	0.37

4.4 Data Analysis

The data analysis showed that regardless of the parameters used, a high foaming ratio resulted in low density. This inverse relationship between the foaming ratio and density is logical, because a higher foaming ratio in a sample means it had better foamability, which resulted in greater pore formation and ultimately reduced the mass of the foamed sample and, as a result, lowers its density.

The more nanoparticles are introduced into the polymer matrix, the higher is the foaming ratio obtained, which results in lower foam density. Therefore, the

addition of NP% has a positive impact on the foamability of the samples. PE polymer had better foaming potential, as it had a much higher foam ratio and much lower foam density when compared to the JSD polymer. Also, as more packing pressure is applied when making the tablets, so a higher foaming ratio is obtained with lower foam density. This trend is also noticeable regarding holding time, foaming temperature and foaming time as shown in Figure 19 and Figure 20. All the parameters exhibited higher foaming ratios and lower foaming densities at the higher levels.

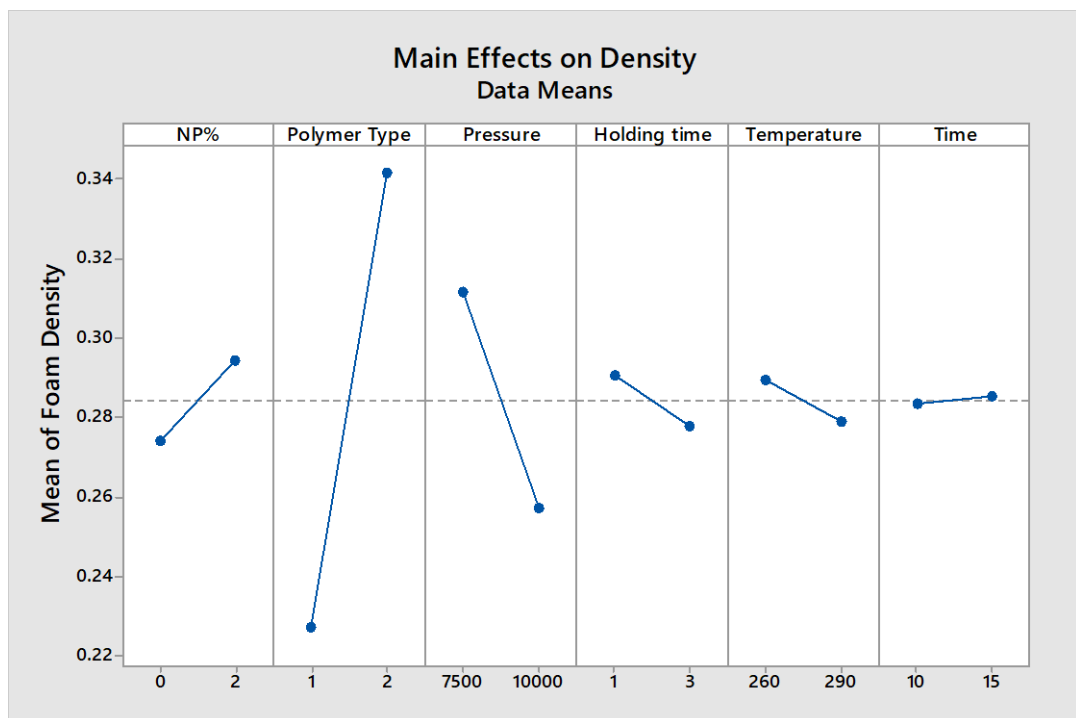


Figure 19: Effect of all parameters on foam density

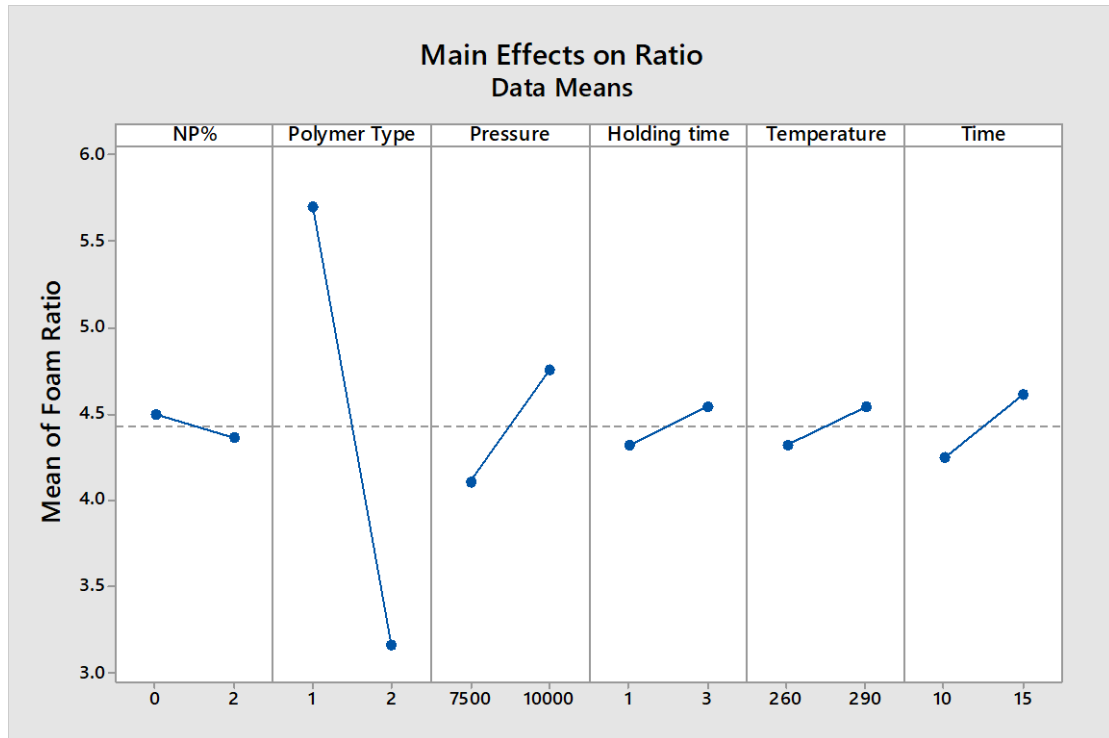


Figure 20: Effect of all parameters on foaming ratio

The table of responses for both foam ratio and foam density are shown in Table 3 and Table 4. In this table we can see that polymer type has the largest effect on both foam density and the foam ratio.

Packing pressure showed only a very small effect on the foam density value, however, its impact was greater on a foam ratio. The NP% had a low impact on the foam density mean value but was ranked as the third most effective factor for foam density. The other factors displayed minimal impact on the foam density mean values.

Table 3: Response table for foam density means

Parameters Level	NP%	Polymer Type	Packing Pressure	Holding Time	Temperature	Foaming Time
1	0.2741	0.0203	0.3115	0.2906	0.2895	0.0105
2	0.2944	0.3415	0.2570	0.2779	0.2790	0.2851
Delta	0.0203	0.1146	0.0546	0.0127	0.0105	0.0017
Rank	3	1	2	5	4	6

Table 4: Response table for foaming ratio means

Parameters Level	NP%	Polymer Type	Packing Pressure	Holding Time	Temperature	Foaming Time
1	4.497	5.703	4.098	4.316	4.314	4.244
2	4.358	3.153	4.758	4.540	4.541	4.611
Delta	0.139	2.550	0.660	0.224	0.227	0.367
Rank	6	1	2	5	4	3

4.5 Confirmation Experiment

According to the Taguchi Analysis, the highest foaming ratio is obtained when Pure PE tablets are prepared with 0% NPs and compressed under a pressure of 10000

LBS. for 3 minutes of holding time and foamed at 290°C for 15 minutes in the oven. The tablets prepared with these factors showed an average foam ratio of 5.38, and an average foam density of 0.261. This is not an optimum result when compared to other experiments. The results are shown in Table 5 and will be discussed separately in Chapter 6.

Table 5: Results of the configuration experiment using parameters recommended by Taguchi analysis

Sample Number	Sample Height	Foam Height	Diameter (mm)	Mass (g)	Volume (cm)	Foam ratio	Foam Density (g/cm ³)
S1	9	49.12	20.46	4.08	16.141	5.45	0.252
S2	9.1	47.44	20.22	4.25	15.22	5.21	0.279
S3	9	49.33	20.44	4.07	16.17	5.48	0.251

Chapter 5: Optimizing Performance

The performance of the samples in this research was evaluated using two different tests: a shape memory test and actuation load measurements. This chapter will discuss the results from each set of experiment in order to suggest the level of each factor that will result in the best possible performance. However, it is important to note that the two properties are independent of one another, and therefore it is not imperative that they both should show their optimum result at the same level.

5.1 Optimizing Shape Memory Effect

Samples for this test were allowed to fully recover their original height, and the recovery time and speed were recorded and calculated in order to study the effect of the different parameters on the shape recovery properties of both the PE and JSD matrices. The results of the calculated recovery speed in mm/min and the recovery time in seconds are shown in Table 6.

Table 6: Average calculated values for recovery speed and time for each experiment

Run #	1	2	3	4	5	6	7	8
Recovery Time (second)	243.66	236	186	188.66	319.33	337.66	170	166.33
Recovery Speed (mm/min)	5.94	6.36	5.16	5.82	5.202	4.68	4.02	4.92

An analysis of the Taguchi Map showed that lower NPs% and packing pressure resulted in faster recovery speeds. On the other hand, longer holding time and higher foaming temperature, with a longer foaming time, recorded higher shape recovery speeds and a lower recovery time. The PE foamed tablets tended to recover faster than the JSD tablets. A summary of the analysis can be found in Figure 21.

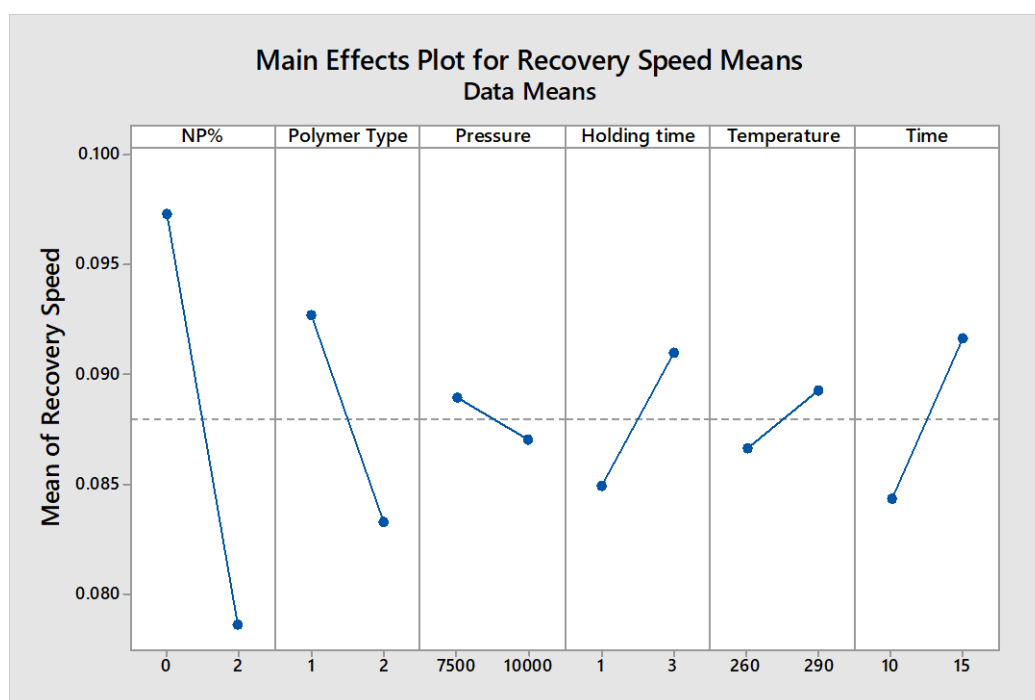


Figure 21: Effect of all parameters on recovery speed of samples

5.1.1 Optimal Shape Memory Effect Based on Taguchi Design

According to the analysis conducted with the Minitab software, the fastest shape recovery can be expected when Pure PE tablets are compressed under 7500 LBS of packing pressure for 3 minutes and foamed at 290°C for 15 minutes. Different sets of three samples were prepared following the recommended levels derived from the Taguchi Analysis. The samples were also compressed to 50% of their original height. The results showed that the average recovery speed for this set

was 7.56 mm/min, with an average recovery time of 158.66 seconds. These results will be discussed in more detail later in the discussion chapter.

5.2 Optimizing Actuation Load

The actuation load is defined as the pushing force exerted by the sample on an object. The samples were placed almost 1 mm away from the force gauge to make a 0.0 N contact force with the force gauge arm. Next, the temperature was increased to 120°C, and kept at that temperature until the sample started to show a decrease in the actuation load. Then, the temperature was allowed to return to room temperature.

The results for the calculated mean value of the maximum actuation load applied by the samples in each experiment can be found in Table 7. The results showed that as NP%, foaming temperature and foaming time increased, higher actuation loads were obtained. Additionally, lower packing pressure increased the actuation load. In this test, the JSD polymer was superior in performance to the PE due to its more rigid structure. A summary of the analysis can be seen in Figure 22.

Table 7: Average measured actuation load values for every experiment

Run #	1	2	3	4	5	6	7	8
Average Maximum Actuation Load (N)	2.36	1.66	0.91	2.35	1.46	0.45	3.01	3.35

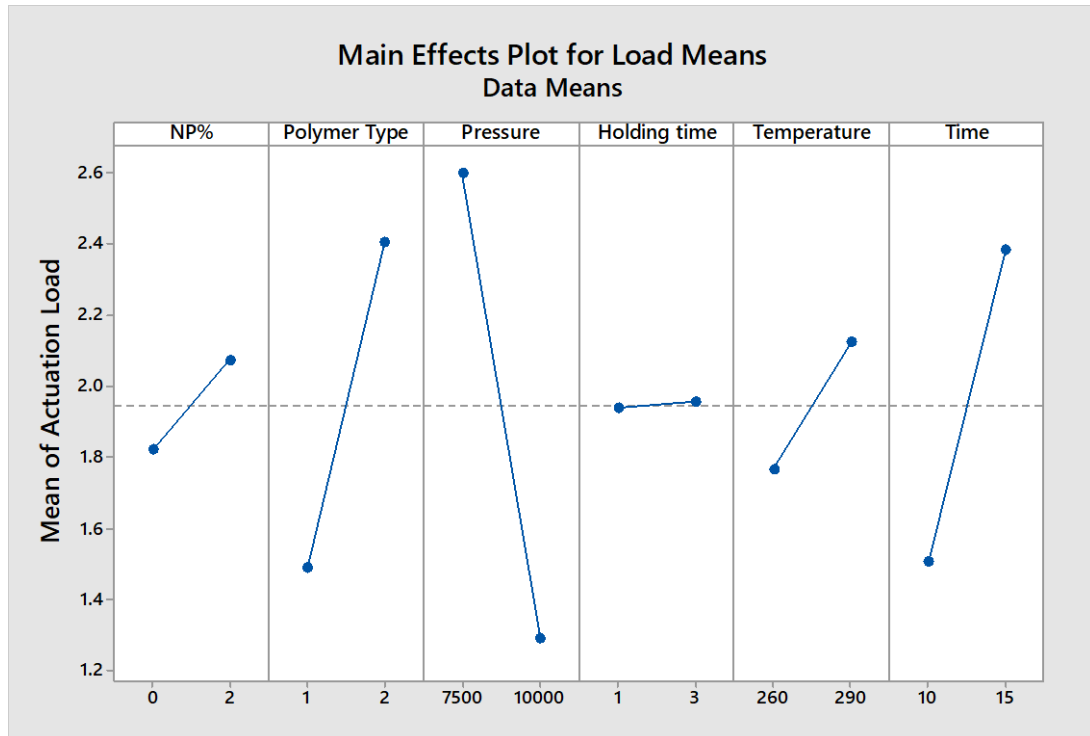


Figure 22: Effect of all parameters on the actuation load

A response table for the actuation load means is shown in Table 8. It is noticeable that packing pressure had the largest effect on the actuation load exerted on the sample, whereas polymer type was the second most effective factor on actuation load.

Foaming time was the third most effective factor. The foaming temperature placed fourth most influential factor on the list. The NP% and holding time gave lowest impact on the actuation force exerted on the sample.

Table 8: Response table for actuation load means

Parameters Level	NP%	Polymer Type	Packing Pressure	Holding Time	Temperature	Foaming Time
1	1.821	1.488	2.600	1.938	1.767	1.508
2	2.071	2.404	1.292	1.954	2.125	2.383
Delta	0.250	0.917	1.308	0.017	0.358	0.875
Rank	5	2	1	6	4	3

5.2.1 Relationship between Actuation Load and Sample Length

A separate test was conducted on six 6 different samples to verify if actuation load is dependent on the sample length. A sample of Pure PE compressed under pressure of 7500 LBS, with 1minute holding time at a temperature of 260°C for a 15 minutes foaming time was prepared. Three (3) of the six (6) samples were machined to a height of 40 mm, whereas the other three (3) were machined to 20 mm height. All the samples were then compressed to 50% of their original height and were ready to be tested.

T-test for equal means was conducted to compare between the mean actuation load of the two samples, Minitab software was used to determine whether the two means were equal or not. Our null hypothesis was that there is no difference between the two means of actuation load with confidence level of 90%. On the other hand, the alternative hypothesis suggested that both means were not equal. Formula used to get t-value is shown below

$$T = \frac{\bar{Y}_1 - \bar{Y}_2}{\sqrt{\frac{s_1^2}{N_1} + \frac{s_2^2}{N_2}}}$$

Where N_1 and N_2 are the sample sizes, \bar{Y}_1 and \bar{Y}_2 are the sample means, and s_1^2 and s_2^2 are the sample variances.

The T-test results showed that there was no effect on the actuation load. T-value of 2.62 was obtained using the formula above. The p-value was 0.142 as shown in MiniTab results below, which is more than the acceptable significance level of $\alpha=0.1$, so null hypothesis is accepted, and the mean values for sample heights 40 mm and 20 mm were considered equal.

Two-Sample T-Test and CI: sample of 40 mm, sample of 20 mm				
Two-sample T for sample of 40 mm vs sample of 20 mm				
	N	Mean	StDev	SE Mean
sample of 40 mm	3	2.650	0.278	0.16
sample of 20 mm	3	2.233	0.126	0.073
Difference = μ (sample of 40 mm) - μ (sample of 20 mm)				
Estimate for difference: 0.417				
90% CI for difference: (-0.098, 0.932)				
T-Test of difference = 0 (vs \neq): T-Value = 2.36 P-Value = 0.142 DF = 2				

5.2.2 Optimal Actuation Load Based on Taguchi Design

According to analysis obtained, the highest actuation load is achieved by a mixture of JSD tablets with 2 wt.% Fe_3O_4 NPs if it is compressed under 7500 LBS of packing pressure for 3 minutes and foamed at 260°C for 15 minutes. Three samples were prepared at the previously mentioned levels, samples were compressed to 50% of their original heights. The recorded average actuation load was 2.48 N. The actuation loads recorded were as follows: 2.45, 2.65 and 2.35 N for samples 1, 2 and 3, respectively. A detailed discussion of these results can be found in Chapter 6.

Figure 23 shows the actuation load curves for all the experiments. Each curve represents an average value for the three samples that were prepared for each experiment. It can be seen that run number 8 had the highest actuation load value of approximately 3.35 N, while run number 7 came second in line with an average maximum actuation load of 3.016 N.

Runs 4, 1, 2, 5 and 3 came 3rd, 4th, 5th, 6th and 7th with average actuation loads of 2.35, 2.36, 1.66, 1.46 and 0.9 N, respectively. Run number 6, however, recorded the lowest average actuation load of all with a value of only 0.45 N. It was observed that all the curves had very similar increment rates, it took every sample a period of around 2 minutes (120 seconds) to reach their maximum actuation load value.

All the samples showed the same reduction behavior after they achieved their maximum actuation load, but none of them reached 0 N by the end. The lowest actuation loads were 0.25 and 0.35 N for runs 3 and 6, respectively, as compared to maximums of 2.68 N for run number 8, and 2.3 N for run number 7.

It is worth mentioning that the samples started to apply actuation loads when the temperature inside the oven was between 80°C and 90°C. After that, temperature had no impact on the actuation loads of the samples.

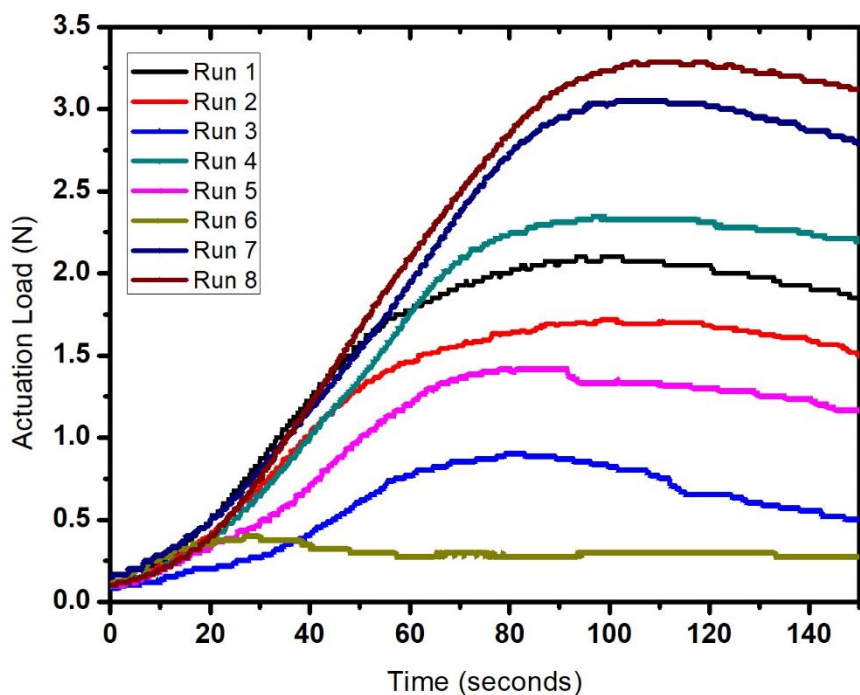


Figure 23: Actuation load curves for each experiment

5.3 Optimum Processing Parameters

The highest foam ratio was obtained when PE+2% NPs tablets were compressed under 10000 LBS of pressure for 1 minute and foamed at 290°C for 15 minutes. The lowest density was obtained with PE+2% NPs tablets compressed under 10000 LBS packing pressure for 3 minutes and foamed at 260°C for 10 minutes.

The fastest shape recovery speed was achieved when Pure PE tablets were prepared and compressed under a pressure of 7500 LBS and a holding time of 3 minutes, before being foamed at 290°C for 15 minutes.

Finally, the highest actuation load was achieved with JSD+2% NPs tablets compressed under a packing pressure of 7500 LBS for a holding time of 3 minutes and foamed at 260°C for 15 minutes.

It is clear that a packing pressure of 7500 LBS is expected not to give highest foam ratio but give high recovery speed and actuation load. If PE tablets are prepared with 2% NPs, foam ratio and density are expected to be positively influenced with expected reduction on recovery speed. Additionally, a greater decrease in the actuation load is to be expected. The optimum holding times for density, recovery speed and actuation load measurement were 3 minutes.

The final factors remaining are foam temperature and foaming time. The optimum values for both were 260°C and 15 minutes, respectively, where they both are expected to positively impact the actuation load and density, with a little increment on shape recovery speed and foam ratio.

These optimum levels were applied to PE polymer with 2% Fe₃O₄ NPs added and compressed with a packing pressure of 7500 LBS for a holding time of 3 minutes. The tablets formed was foamed at 260°C for 15 minutes.

The results as shown in Table 9 were obtained from averages of the three samples. The foam ratio obtained was the 2nd highest and the density was the 4th lowest relative to all the experiments. The average recovery speed was 4th fastest at 5.76 mm/min from the fastest recovery speed recommended by the Taguchi Analysis levels for SME. The actuation load had the 4th highest value of 2.06 N, while the highest value was 3.35 N for JSD+2% NPs.

Table 9: Values of foaming ratio, density, recovery speed and actuation load of tablets prepared under optimum levels

Average Foam Ratio	Average Foam Density (g/cm ³)	Average Recovery speed (mm/min)	Average Actuation Load (N)
6.16	0.24	5.76	2.06

Chapter 6: Discussion

This chapter aims to discuss the findings of this research and shows a summary of the data collected from the conducted experiments. Observations and measurements taken whilst experimenting will also be mentioned in this chapter. Results obtained from foaming temperature determination experiment will be discussed here, as well as foaming ratio and density measurements results, in addition to the performance testing experiments namely, shape memory effect and actuation load tests. Finally, a discussion about the optimum parameters test will be initiated.

6.1 Foaming Temperature Determination

Before starting the foaming process, it was essential to decide which foaming temperatures are to be chosen. These values had to be less than burning temperature of the polymer to avoid damaging the sample, and more than glass transition temperature (T_g) of the polymer. For that to be ascertained DSC was operated on both polymers and graphs obtained can be found in Figure 24 and Figure 25.

The analysis of the DSC graphs was carried out using TRIOS software, T_g of pure PE was 78.1°C whereas T_g for JSD was at around 75°C. DSC runs were operated at maximum temperature value of 250°C in all runs and in none of these runs showed melting temperature curve.

The ratios measured at 260°C and 290°C were the highest measured ratios from all the temperatures. High ratio obtained indicates that the tablet foamed properly, and large pores were generated within the polymer matrix. This can be

attributed to the motion of the polymer chains within the matrix, as they had more freedom at higher temperatures, which allowed the chains to move away from each other and make larger pores.

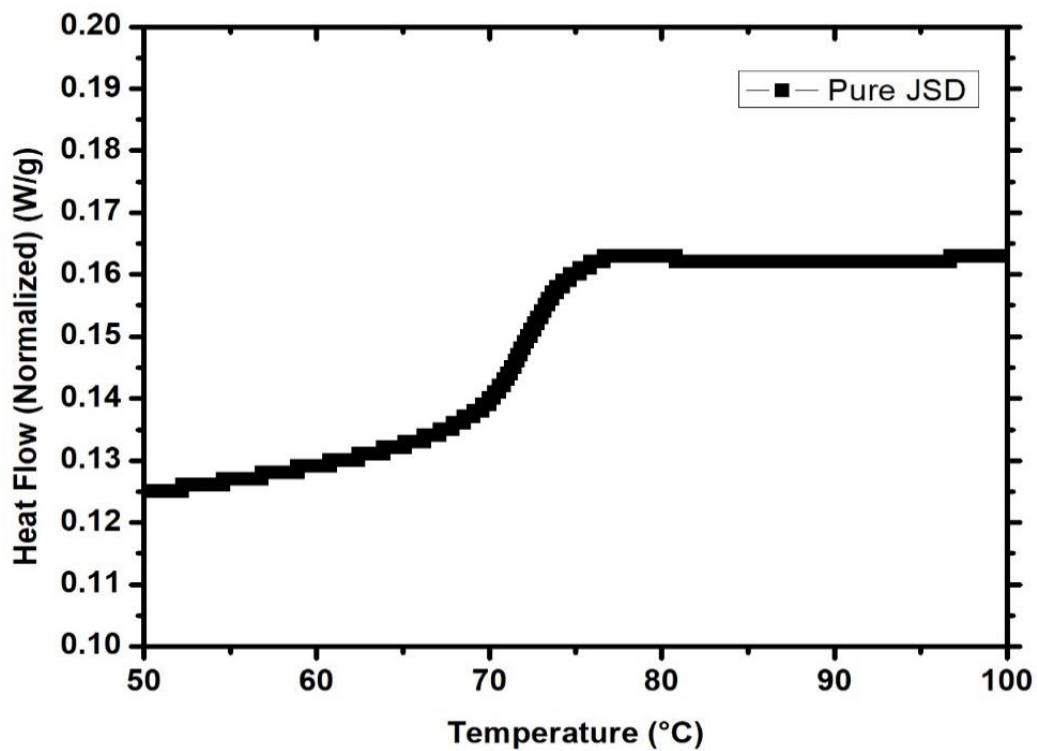


Figure 24: DSC run of Pure JSD

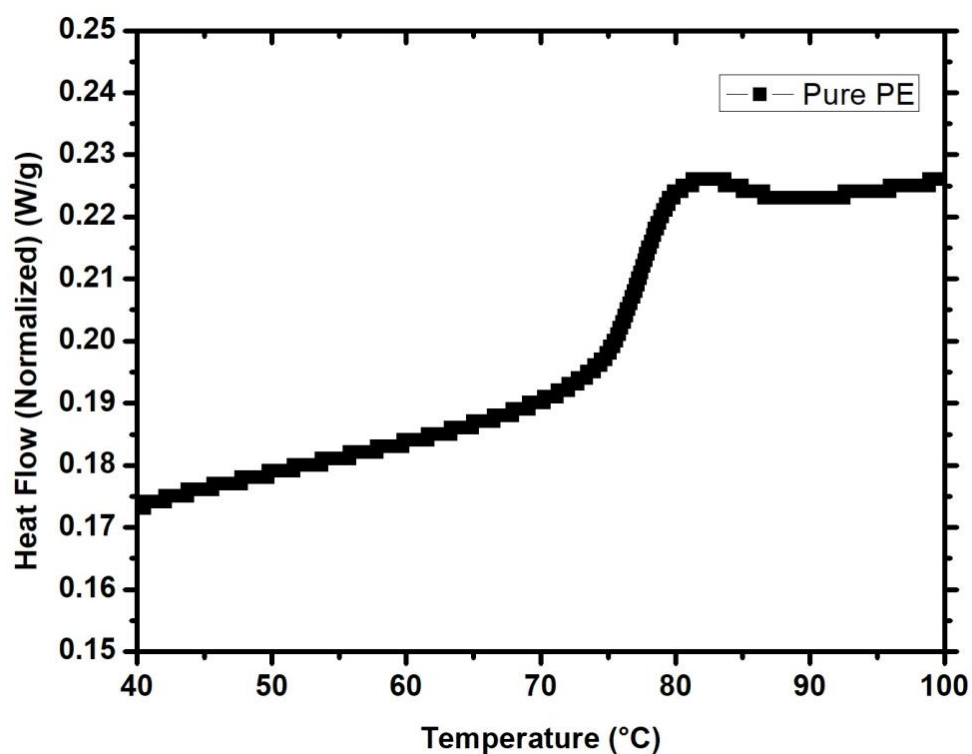
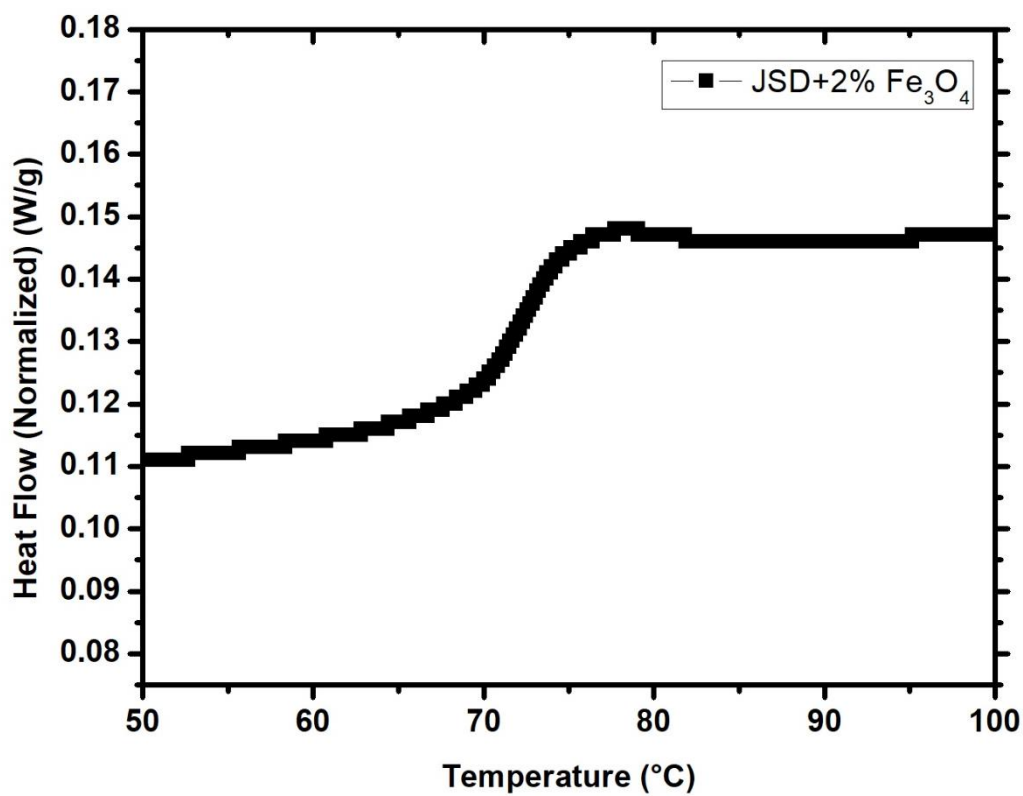
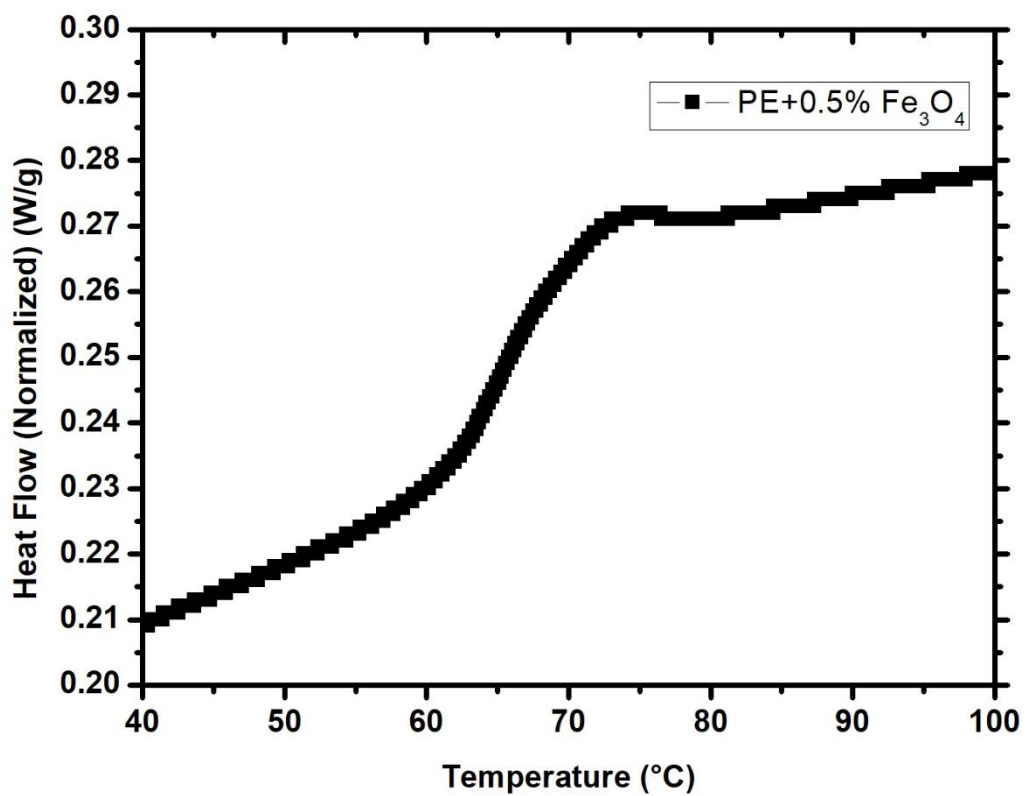


Figure 25: DSC run of pure PE

Not only foaming temperature levels were selected using this test, but also the NPs%. Another DSC run was operated on PE with 0.5% Fe_3O_4 and JSD with 2% Fe_3O_4 . Results are shown in Figure 26 and Figure 27. It is clear from PE graph that only 0.5% Fe_3O_4 reduced T_g down to 72.81°C. On the other hand, JSD's T_g was not affected even when 2% Fe_3O_4 was added to its matrix and it was around 74.92°C. The drop in T_g value for PE polymer is attributed to the enhancement of chains motion was enhanced because of plasticization effect of Fe_3O_4 nanoparticules, and also because Fe_3O_4 transferred the heat more efficiently into PE matrix. T_g value for JSD remained the same and that is because Fe_3O_4 NPs seem to not enhance heat transfer within the polymer matrix.

Figure 26: DSC graph of JSD + 2 w.t% Fe₃O₄Figure 27: DSC graph of PE + 0.5 w.t% Fe₃O₄

These DSC runs helped to select NP% levels of 0% and 2%. A test was conducted on the effect of NP% on shape recovery speed of PE polymer. Results as in Figure 28 showed that any further increment in NPs concentration will have a negative impact on the recovery speed of the matrix. This decrement in the recovery speed is due to the existence of discontinuous phase (nanoparticles) inside PE matrix which results in stopping the shape recovery process as nanoparticles themselves do not recover their shape and thus their existence makes it harder for the sample to properly show its shape memory property. Thus, best levels for NP% was 0% and 2%. This conclusion can be extended about the JSD polymer; it is expected not to show any improvement beyond the 2% of Fe_3O_4 . So, in conclusion these two percentages of Nanoparticles were selected.

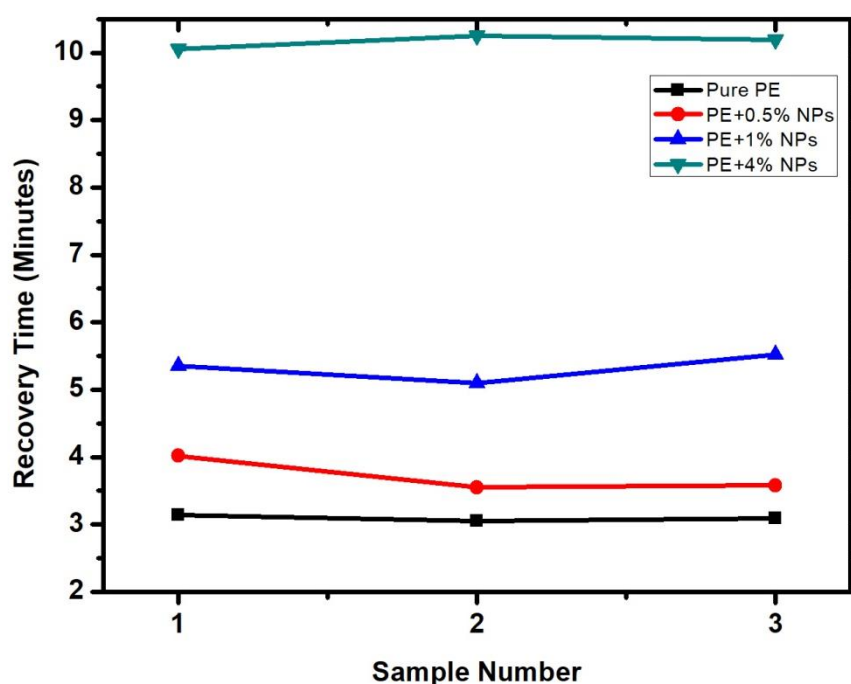


Figure 28: Shape recovery time of PE polymer at different NPs concentrations

6.2 Foaming Ratio and Density Measurements

Process parameters are expected to have the same effect on foaming ratio and density; increasing foaming ratio leads to decreasing their density. This is valid unless the NP are added; if the polymer contains NP, the foaming ratio improved, but the density not necessarily decreases, simply because the NP density increases the composite density. Quadrini et al. (2010) studied the impact of adding nanoclays to resin powder foamed samples. Obtained results showed that addition of nanoclays reduced foam ratio and increased foam density. This is expected because addition of nanoclays reduced volume percentage and less resin was present in the composition.

From Table 3 and Table 4, polymer type and packing pressure were the most influencing factors on both density and foam ratio of samples which indicates that these properties depend on the material used as well as how much that material is compressed. More pressure causes the powder to be more compacted and connected, thus results in better heat transfer within the structure itself.

Temperature and holding time were 4th and 5th most effecting factors. Ultimately more temperature helped polymer chains to move freely and was recommended to obtain higher foam ratio and lower foam density.

NP% showed significant impact (10%) on the foam density as well as the observed foaming ratio when it was added to PE, it is expected as mentioned before that any increment in NP% will improve heat transfer within the PE polymer matrix and thus give higher foam ratio and lower density. However, the same significance was not obtained when the NP is added to JSD. PE polymer showed very high ratios of 5.95 when NPs were added compared to 5.44 at 0% of NP as shown in Table 2.

On the other hand, JSD showed lower ratios 2.75 compared to 3.54 at 0% of NP; this result is not consistent with the expected outcome, (NP addition supposed to improve formality). Careful investigation of this phenomenon led to the fact that foaming temperature working range had dependency on the polymer type. Hence a new experiment was conducted to verify this effect, foaming temperature of 240°C was performed and the resulted foaming ratio was 3.8, it indicates an improvement of (7%) compared to 0% NPs.

It can be concluded that the effect of foaming temperature is dependent on the polymer type. Due to this dependency, the optimal design suggested by Taguchi analysis was not optimal. Further tuning of the Taguchi parameters was performed. The below two sections discuss the results obtained from optimal factor suggested by Taguchi and the modified optimal factors based on experimental observation.

6.2.1 Optimal Ratio and Density Based on Taguchi Design

Three samples were prepared under the suggested Taguchi levels, the average foam ratio was ranked 4th. Since this is not the optimal, further tuning of the suggested parameters is required. This action is required for Taguchi design whenever the independency assumption is violated. Summary of the suggested levels from Taguchi design are shown in Table 10.

Table 10: Taguchi design of process parameter for optimal ratio and density

Process parameter	Value	unit
NP%	0%	N/A
Polymer Type	PE	N/A
Packing Pressure	10000	LBS
Holding Time	3	minutes
Foaming Temperature	290	°C
Foaming Time	15	minutes

6.2.2 Modified Optimal Suggested by Taguchi

As discussed above, there is a dependency effect between the polymer type and the foaming temperature; Thus, one experiment with three replicate samples was conducted, this experiment has all suggested levels by Taguchi, except the NP% is selected to be 2% as that is expected to show better results. Foam ratio obtained from this experiment was the highest among all experiments done at a value of 7.02 and the measured density of 0.211 was the second lowest compared to all other experiments.

6.3 Shape Memory Effect

It is defined as the ability of a sample to retrieve its original shape after being deformed. This test was operated on each sample to measure its shape recovery

speed. Recovery speed is obtained from dividing its recovered height by its recovery time. As shown in Figure 21, the fastest recovery speed was achieved when no NPs were added to the polymer matrix; refer to Table 11 for results.

Table 11: Effect of NP% on the recovery speed (mm/minute)

Polymer type \ NP%	PE	JSD	Average
0%	5.97	5.5	5.735
2%	4.92	4.47	4.695
Average	5.445	4.985	5.215

This is attributed to the fact that addition of NPs although transfers heat more efficiently into the matrix, it creates discontinuity in the polymer matrix and causes the sample to take longer time to recover its original height, and thus slower recovery speed. This observation is aligned with observations noted by Gunes et al. (2008); they have observed that silicon carbide (SiC) nano-particles damaged the SME of shape memory epoxy and shape memory polyurethane (SMPU), this negative impact was ascribed to the dramatic decrement of soft segment crystallinity of SMPU.

It is also noticed that holding time under packing pressure has negligible effect on the recovery speed as shown in Table 12.

Table 12: Effect of packing pressure on the recovery speed

Packing pressure \ Holding time	7500	10000	Average
1	5.94	5.16	5.55
3	5.82	6.0	5.91
Average	5.88	5.58	5.73

6.3.1 Optimal Shape Memory Effect Based on Taguchi Design

The recommended levels of process parameters based on Taguchi analysis were tested empirically. Results were found to be optimal; the measured recovery speed was 7.56 mm/min which is the fastest amongst all samples. The PE matrix showed faster recovery due to the existence of TGIC as a crosslinker which improves the recovery process of the matrix. The set of the optimal parameters are shown in Table 13.

Table 13: Taguchi design of process parameter for optimal SME

Process parameter	Value	unit
NP%	0%	N/A
Polymer Type	PE	N/A
Packing Pressure	7500	LBS
Holding Time	3	minutes
Foaming Temperature	290	°C
Foaming Time	15	minutes

6.4 Actuation Load Measurement

Actuation load is the force applied by foamed samples on an object. JSD polymer had a very high actuation load compared to PE, this is attributed to the fact that JSD has higher yield strength compared to PE as shown in Figure 29. Moreover, the foamed JSD is denser than PE (0.29 g/cm^3 compared to 0.25 g/cm^3). Figure 31 demonstrates this fact; the volume of foamed 5 grams of PE is bigger than the volume of 5 grams of JSD, that means JSD is denser than PE, and hence it is capable to exert more actuation load.

It is worth mentioning that addition of NPs to both polymers matrices caused a reduction in compression of both polymers, this is due to the fact that Fe_3O_4 NPs added discontinuity within the structure of the foamed sample, and thus made it easier to break when applying a compression force on it. This trend is shown in Figure 30.

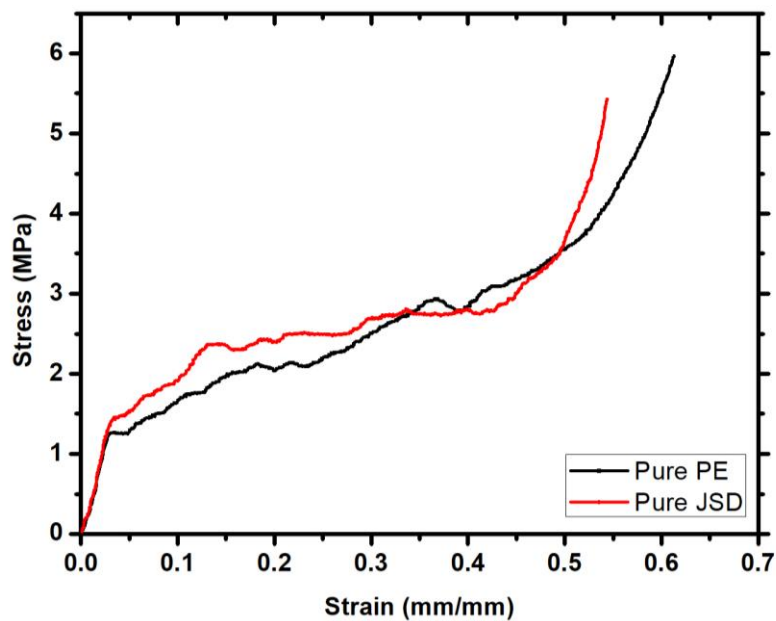


Figure 29: Stress strain graph for both pure PE and pure JSD

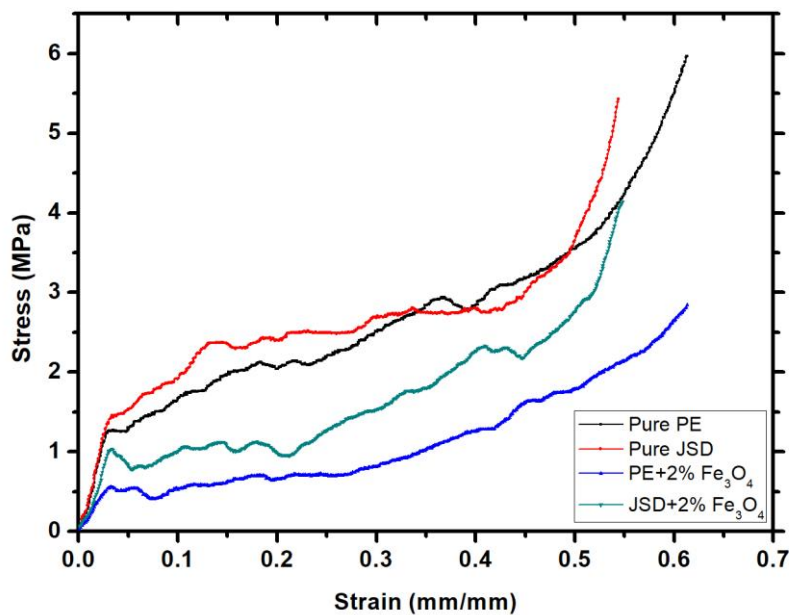


Figure 30: Effect of NPs addition on the compressibility of the samples

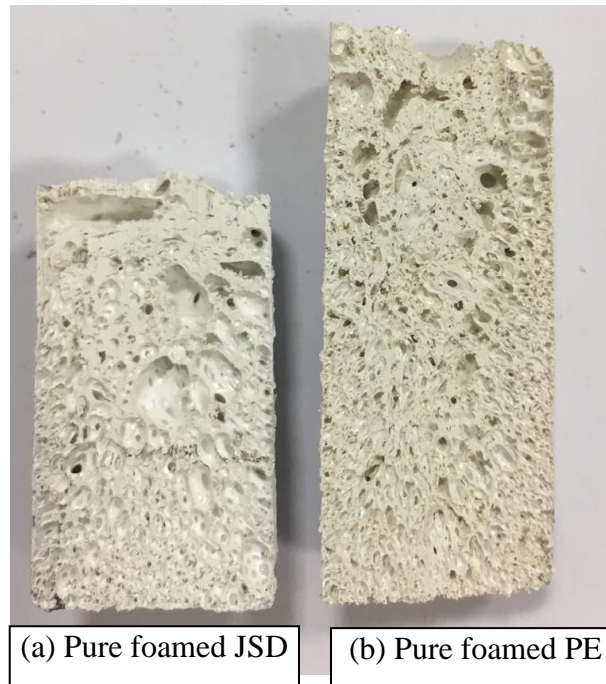


Figure 31: Foamed samples

Samples started exerting actuation load on the force gauge once it reached a temperature between 80°C and 90°C. This temperature is just above T_g of both polymers, refer to Figure 24 and Figure 25 for DSC curves.

The results showed that after T_g temperature was exceeded no effect on the actuation load has been noticed. Further increment did not indicate any increase in the actuation load. The conclusion here is that heat is only needed to trigger and stimulate the sample to recover its original shape.

A similar test has been conducted by Weng et al. (2018) on compressive strength of polyimide/ Fe_3O_4 composite foam, their results showed increment of compressibility of the foam after the addition of NPs. The contradiction between our results is attributed to the fact that the addition of NPs to polyimide was before the polymerization process, which helped NPs to be bonded with the polymer matrix. Thus, had a positive impact on the compressive properties.

6.5 Overall Optimum Processing Parameters

In this process NP%, polymer type, packing pressure, holding time, foaming temperature and foaming time parameters were selected to obtain best possible overall performance. The selected parameters can be found in Table 14.

NP% and Polymer Type

Addition of 2% Fe₃O₄ into PE polymer matrix provided better heat conducting efficiency where its effect was noticed when foam ratio was measured to be 6.16 which was the 2nd highest measured ratio of all experiments and 0.241 g/cm³ density to be the 4th lowest density measured with not much difference between that and the lowest one at a value of 0.20 for experiment number 6.

Packing Pressure and Holding Time

Although, Packing pressure of 7500 LBS and 3 minutes holding time allowed tablets to be connected just enough not to be broken or brittle and to form good shaped foam which provided more freedom once subjected to heat, but the existence of Fe₃O₄ within PE matrix resulted in a discontinuity between its chains which had a negative impact on the recovery speed of the foamed samples, the calculated average recovery speed for the prepared samples of 5.76 mm/min was still not slow compared to 6.36 mm/min fastest recovery speed obtained from experiment number 2 and that makes the considered levels optimum to process good behaving samples.

Average actuation load recorded was 2.06 N which was 4th highest compared to all other experiments, the resultant load was expected to be of that value because PE polymer matrix did not have an uniformly distributed pores within its matrix

because of the existent discontinuous phase which impacts the actuation load delivered by the sample.

Foaming Temperature and Foaming Time

The selected foaming temperature and foaming time played important role in obtaining relatively high ratio as it helped the polymer chains to move more freely and generate foam within the polymer's structure.

Table 14: Selected optimum parameters levels

Optimized responses Parameter	Foaming ratio	Shape recovery speed	Actuation load	Selected level
NP%	2%	0%	2%	2%
Polymer type	PE	PE	JSD	PE
Packing pressure (LBS)	10000	7500	7500	7500
Holding time (Minutes)	1	1	3	3
Foaming temperature (°C)	290	260	260	260
Foaming time (Minutes)	15	15	15	15

Chapter 7: Conclusion

Solid state foaming process with no foaming agent was tested on 2 different polymers namely Corro-Coat PE Series 7 (PE) and Jotun Super Durable 2903 (JSD). Tablets of the mentioned above polymers were processed and prepared under different levels of packing pressure, holding time and nanoparticles concentration. The prepared tablets were foamed under different levels of foaming temperature and foaming time. Different tests were conducted on these foamed samples to measure their foaming ratios, densities, shape recovery speed and actuation load.

- **Foaming Process:**

- PE polymer powder has better tendency to show higher foaming ratios and lower density compared to JSD due to the existence of TGIC crosslinks within its matrix.
- NP% allows better conductivity of heat within PE matrix and thus easier motion around the netpoints which increases the foaming ratio. On the other hand, it gave negative impact when added to JSD at higher temperature. This is attributed to the fact that NPs are heavier than the polymer powder and thus forced it not to move freely. A positive impact was observed at foaming temperature of 240°C.

- **SME Performance:**

- Shape recovery speed was mostly affected by packing pressure; low packing pressure gives higher recovery speed.
- Insertion of NPs within the polymer matrix did not help to increase shape recovery speed. In fact, it caused it to reduce; this is because NPs do not possess shape memory behavior in their nature, and because they caused discontinuity within the polymer matrix.

- **Actuation Load:**

- JSD polymer matrix showed improvement in actuation load values when NPs were introduced to its matrix.
- Addition of NPs created discontinuity within the foamed sample structure and as a result; made it brittle and easier to break.

- **Overall Optimum:**

- The proposed optimum process parameters to obtain optimum results from all tests are as following: PE polymer mixed with 2% Fe₃O₄ NPs compressed under a pressure of 7500 LBS for 3 minutes holding time and foamed at 260°C for 15 minutes foaming time.
- Foam ratio obtained was 6.16 and density was 0.267 g/cm³
- The calculated average recovery speed was 5.76 mm/min.
- The measured actuation load had the value of 2.06 N.

- **Future Work:**

- Further pores expansion techniques can be tested for bigger pore size and better uniform size distribution. These techniques could be rotational or ultrasonic vibration
- Conducting the foaming process under vacuum could improve the foaming process by increasing the pore size and stabilize the final foal structure.
- Study the foaming process with time: perform the foaming process under specific heating curve (e.g, cyclic heat load)
- Further material characterization will be operated to obtain deeper knowledge of the chemical composition, structural properties and morphology of the foamed samples before and after addition of NPs.

References

- Abdullah, S. I., & Ansari, M. N. M. (2015). Mechanical properties of graphene oxide (GO)/epoxy composites. *HBRC Journal*, *11*(2), 151–156.
<https://doi.org/10.1016/j.hbrcj.2014.06.001>
- Ahmed, M. F., Li, Y., Yao, Z., Cao, K., & Zeng, C. (2019). TPU/PLA blend foams: Enhanced foamability, structural stability, and implications for shape memory foams. *Journal of Applied Polymer Science*, *136*(17), 47416.
<https://doi.org/10.1002/app.47416>
- Boxall, C., Kelsall, G., & Zhang, Z. (1996). Photoelectrophoresis of colloidal iron oxides. Part 2.—Magnetite (Fe_3O_4). *Journal of the Chemical Society, Faraday Transactions*, *92*(5), 791–802.
<https://doi.org/10.1039/FT9969200791>
- Cornell, R. M., & Schwertmann, U. (2003). *The iron oxides: Structure, properties, reactions, occurrences, and uses* (2nd, completely rev. and extended ed ed.). Weinheim: Wiley-VCH.
- Dorigato, A., Biani, A., Bonani, W., & Pegoretti, A. (2019). Thermo-electrical behaviour of cyclic olefin copolymer/exfoliated graphite nanoplatelets nanocomposites foamed through supercritical carbon dioxide. *Journal of Cellular Plastics*, *55*(3), 263–282.
<https://doi.org/10.1177/0021955X19839733>
- Fabrizio, Q., Loredana, S., & Anna, S. E. (2012). Shape memory epoxy foams for space applications. *Materials Letters*, *69*, 20–23.
<https://doi.org/10.1016/j.matlet.2011.11.050>
- Gu, S.-Y., Chang, K., & Jin, S.-P. (2018). A dual-induced self-expandable stent based on biodegradable shape memory polyurethane nanocomposites (PCLAU/ Fe_3O_4) triggered around body temperature: Research Article. *Journal of Applied Polymer Science*, *135*(3), 45686.
<https://doi.org/10.1002/app.45686>
- Gunes, I. S., Cao, F., & Jana, S. C. (2008). Evaluation of nanoparticulate fillers for development of shape memory polyurethane nanocomposites. *Polymer*, *49*(9), 2223–2234. <https://doi.org/10.1016/j.polymer.2008.03.021>

- Hager, M. D., Bode, S., Weber, C., & Schubert, U. S. (2015). Shape memory polymers: Past, present and future developments. *Progress in Polymer Science*, 49–50, 3–33. <https://doi.org/10.1016/j.progpolymsci.2015.04.002>
- Huang, W. M., Song, C. L., Fu, Y. Q., Wang, C. C., Zhao, Y., Purnawali, H., ... Zhang, J. L. (2013). Shaping tissue with shape memory materials. *Advanced Drug Delivery Reviews*, 65(4), 515–535. <https://doi.org/10.1016/j.addr.2012.06.004>
- Ito, A., Semba, T., Taki, K., & Ohshima, M. (2014). Effect of the molecular weight between crosslinks of thermally cured epoxy resins on the CO₂-bubble nucleation in a batch physical foaming process. *Journal of Applied Polymer Science*, 131(12), n/a-n/a. <https://doi.org/10.1002/app.40407>
- Kausar, A. (2018). Polyurethane Composite Foams in High-Performance Applications: A Review. *Polymer-Plastics Technology and Engineering*, 57(4), 346–369. <https://doi.org/10.1080/03602559.2017.1329433>
- Kulkarni, S. A., Sawadh, P. S., Palei, P. K., & Kokate, K. K. (2014). Effect of synthesis route on the structural, optical and magnetic properties of Fe₃O₄ nanoparticles. *Ceramics International*, 40(1), 1945–1949. <https://doi.org/10.1016/j.ceramint.2013.07.103>
- Matuana, L. M., Faruk, O., & Diaz, C. A. (2009). Cell morphology of extrusion foamed poly(lactic acid) using endothermic chemical foaming agent. *Bioresource Technology*, 100(23), 5947–5954. <https://doi.org/10.1016/j.biortech.2009.06.063>
- Quadrini, F., & Squeo, E. A. (2008). Solid-State Foaming of Epoxy Resin. *Journal of Cellular Plastics*, 44(2), 161–173. <https://doi.org/10.1177/0021955X07082486>
- Ratna, D., & Karger-Kocsis, J. (2008). Recent advances in shape memory polymers and composites: A review. *Journal of Materials Science*, 43(1), 254–269. <https://doi.org/10.1007/s10853-007-2176-7>
- Santo, L. (2014). Recent Developments in the Field of Shape Memory Epoxy Foams. *Materials Science Forum*, 783–786, 2523–2530. <https://doi.org/10.4028/www.scientific.net/MSF.783-786.2523>
- Santo, L. (2016). Shape memory polymer foams. *Progress in Aerospace Sciences*, 81, 60–65. <https://doi.org/10.1016/j.paerosci.2015.12.003>

- Santo, L., Quadrini, F., Squeo, E. A., Dolce, F., Mascetti, G., Bertolotto, D., ... Zolesi, V. (2012). Behavior of Shape Memory Epoxy Foams in Microgravity: Experimental Results of STS-134 Mission. *Microgravity Science and Technology*, 24(4), 287–296. <https://doi.org/10.1007/s12217-012-9313-x>
- Santo, L., Tedde, G. M., & Quadrini, F. (2015). Manufacturing of a Shape Memory Polymer Actuator. *Volume 1: Processing*, V001T02A055. <https://doi.org/10.1115/MSEC2015-9313>
- Soto, G. D., Meiorin, C., Actis, D. G., Mendoza Zélis, P., Moscoso Londoño, O., Muraca, D., ... Marcovich, N. E. (2018). Magnetic nanocomposites based on shape memory polyurethanes. *European Polymer Journal*, 109, 8–15. <https://doi.org/10.1016/j.eurpolymj.2018.08.046>
- Squeo, E. A., & Quadrini, F. (2010). Shape memory epoxy foams by solid-state foaming. *Smart Materials and Structures*, 19(10), 105002. <https://doi.org/10.1088/0964-1726/19/10/105002>
- Taguet, A., Cassagnau, P., & Lopez-Cuesta, J.-M. (2014). Structuration, selective dispersion and compatibilizing effect of (nano)fillers in polymer blends. *Progress in Polymer Science*, 39(8), 1526–1563. <https://doi.org/10.1016/j.progpolymsci.2014.04.002>
- Vialle, G., Di Prima, M., Hocking, E., Gall, K., Garmestani, H., Sanderson, T., & Arzberger, S. C. (2009). Remote activation of nanomagnetite reinforced shape memory polymer foam. *Smart Materials and Structures*, 18(11), 115014. <https://doi.org/10.1088/0964-1726/18/11/115014>
- Wang, J., Luo, J., Kunkel, R., Saha, M., Bohnstedt, B. N., Lee, C.-H., & Liu, Y. (2019). Development of shape memory polymer nanocomposite foam for treatment of intracranial aneurysms. *Materials Letters*, 250, 38–41. <https://doi.org/10.1016/j.matlet.2019.04.112>
- Wang, Y., Ye, J., & Tian, W. (2016). Shape Memory Polymer Composites of Poly(styrene-*b*-butadiene-*b*-styrene) Copolymer/Liner Low Density Polyethylene/Fe₃O₄ Nanoparticles for Remote Activation. *Applied Sciences*, 6(11), 333. <https://doi.org/10.3390/app6110333>
- Weng, L., Wang, T., Ju, P.-H., & Liu, L.-Z. (2018). Preparation and properties of polyimide/Fe₃O₄ composite foams. *Pigment & Resin Technology*, 47(2), 173–179. <https://doi.org/10.1108/PRT-01-2017-0006>

- Wu, S., Sun, A., Zhai, F., Wang, J., Xu, W., Zhang, Q., & Volinsky, A. A. (2011). Fe₃O₄ magnetic nanoparticles synthesis from tailings by ultrasonic chemical co-precipitation. *Materials Letters*, *65*(12), 1882–1884.
<https://doi.org/10.1016/j.matlet.2011.03.065>
- Wu, W., Wu, Z., Yu, T., Jiang, C., & Kim, W.-S. (2015). Recent progress on magnetic iron oxide nanoparticles: Synthesis, surface functional strategies and biomedical applications. *Science and Technology of Advanced Materials*, *16*(2), 023501. <https://doi.org/10.1088/1468-6996/16/2/023501>
- Wypych, G. (2016). *Handbook of Fillers*. Elsevier.
- Yang, J., Liao, X., Li, J., He, G., Zhang, Y., Tang, W., ... Li, G. (2019). Light-weight and flexible silicone rubber/MWCNTs/Fe₃O₄ nanocomposite foams for efficient electromagnetic interference shielding and microwave absorption. *Composites Science and Technology*, *181*, 107670.
<https://doi.org/10.1016/j.compscitech.2019.05.027>
- Yao, Y., Zhou, T., Xu, Y., Liu, Y., & Leng, J. (2018). Preparation and characterization of shape memory composite foams based on solid foaming method. *Journal of Applied Polymer Science*, *135*(46), 46767.
<https://doi.org/10.1002/app.46767>
- Zhang, H., Zhang, G., Li, J., Fan, X., Jing, Z., Li, J., & Shi, X. (2017). Lightweight, multifunctional microcellular PMMA/Fe₃O₄@MWCNTs nanocomposite foams with efficient electromagnetic interference shielding. *Composites Part A: Applied Science and Manufacturing*, *100*, 128–138.
<https://doi.org/10.1016/j.compositesa.2017.05.009>
- Zheng, X., Zhou, S., Xiao, Y., Yu, X., Li, X., & Wu, P. (2009). Shape memory effect of poly(d,l-lactide)/Fe₃O₄ nanocomposites by inductive heating of magnetite particles. *Colloids and Surfaces B: Biointerfaces*, *71*(1), 67–72.
<https://doi.org/10.1016/j.colsurfb.2009.01.009>
- Zhou, Y., & Huang, W. M. (2015). Shape Memory Effect in Polymeric Materials: Mechanisms and Optimization. *Procedia IUTAM*, *12*, 83–92.
<https://doi.org/10.1016/j.piutam.2014.12.010>